Oscialltions of Neutron-Star Merger Remnants

Andreas Bauswein

(Heidelberg Institute for Theoretical Studies)

with N. Stergioulas, J. Clark, H.-T. Janka

NewCompStar Meeting on Oscillations and Instabilities of neutron stars

Southampton, 14/09/2016

Heidelberg Institute for Theoretical Studies

HITS

comp star

Outline

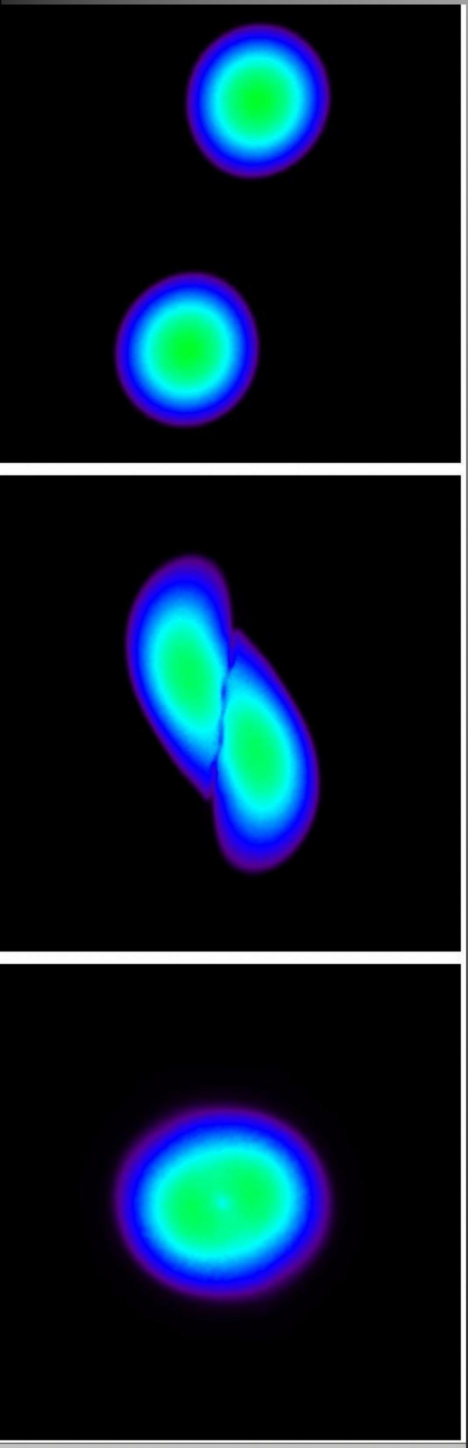

- Merger remnant as oscillating, rotating neutron star?
- Dominant postmerger oscillation
- Origin of secondary (GW) features
- Classification of postmerger GW emission and dynamics
- Dependencies of frequencies
- Model for postmerger GW emission

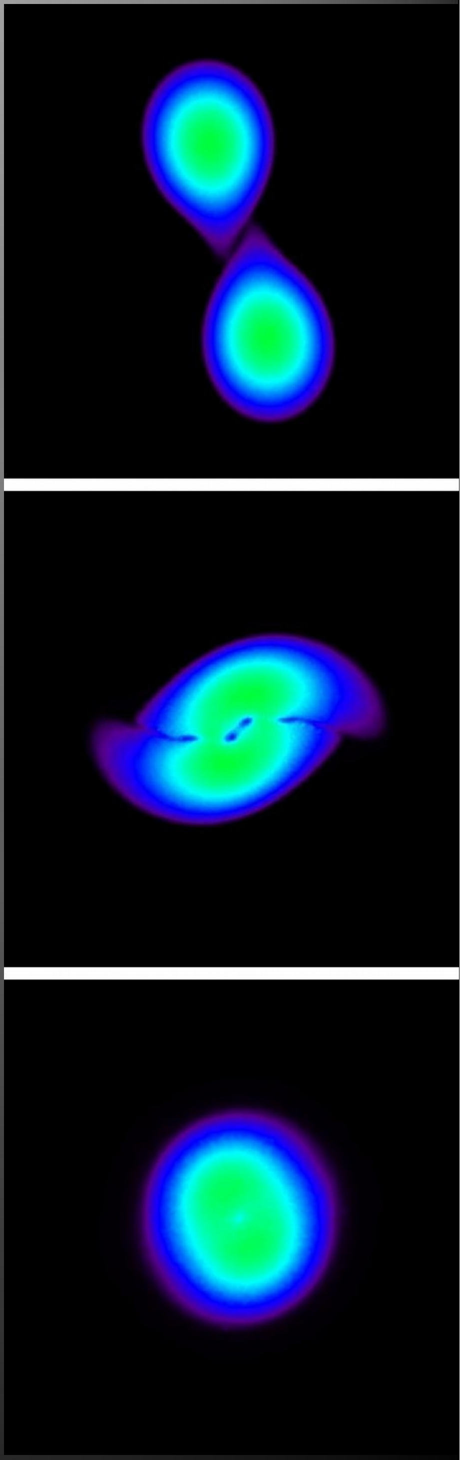

Generic GW spectrum

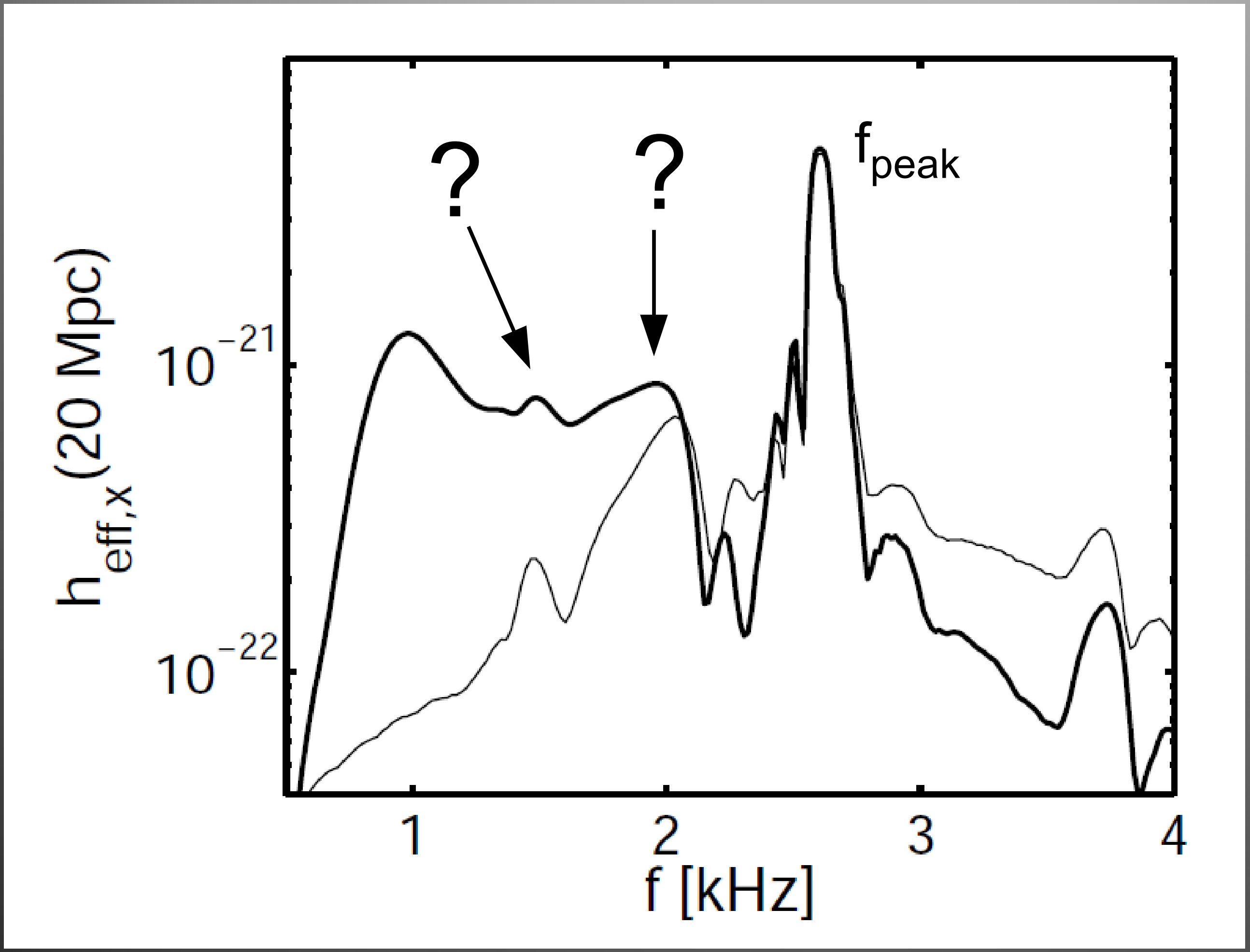

Thin line postmerger only

Note: no unique nomenclature in the literature, e.g. f_{peak} is also called f_2 ...

- Up to three pronounced features in the postmerger spectrum (+ structure at higher frequencies)
- Simulation: 1.35-1.35 M_{sun} DD2 EoS, Smooth Particle Hydro, Conformal Flatness
- Generic in the sense that not all secondary peaks are necessarily present

Dominant oscillation frequency

- Robust feature, which occurs in all models (which don't collapse promptly to BH)
- Fundamental quadrupolar fluid mode of the remnant

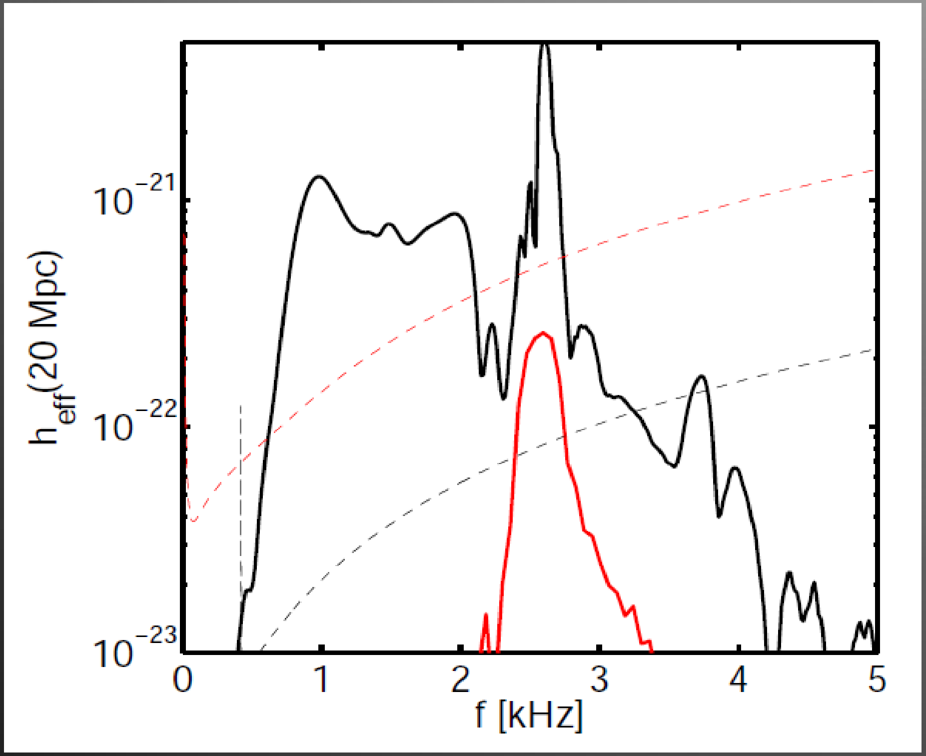

Re-excitation of f-mode (l=|m|=2) in late-time remnant (Bauswein et al. 2016)

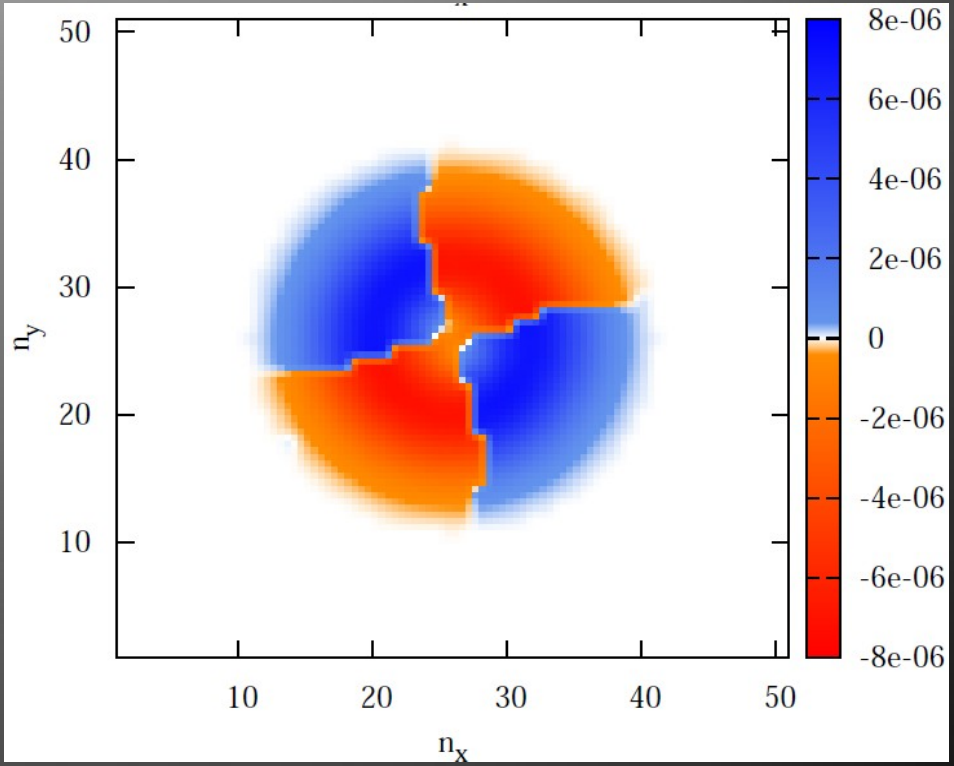

Mode analysis at $f=f_{peak}$
Stergioulas et al. 2011

Lapse function:

Rest-mass density:

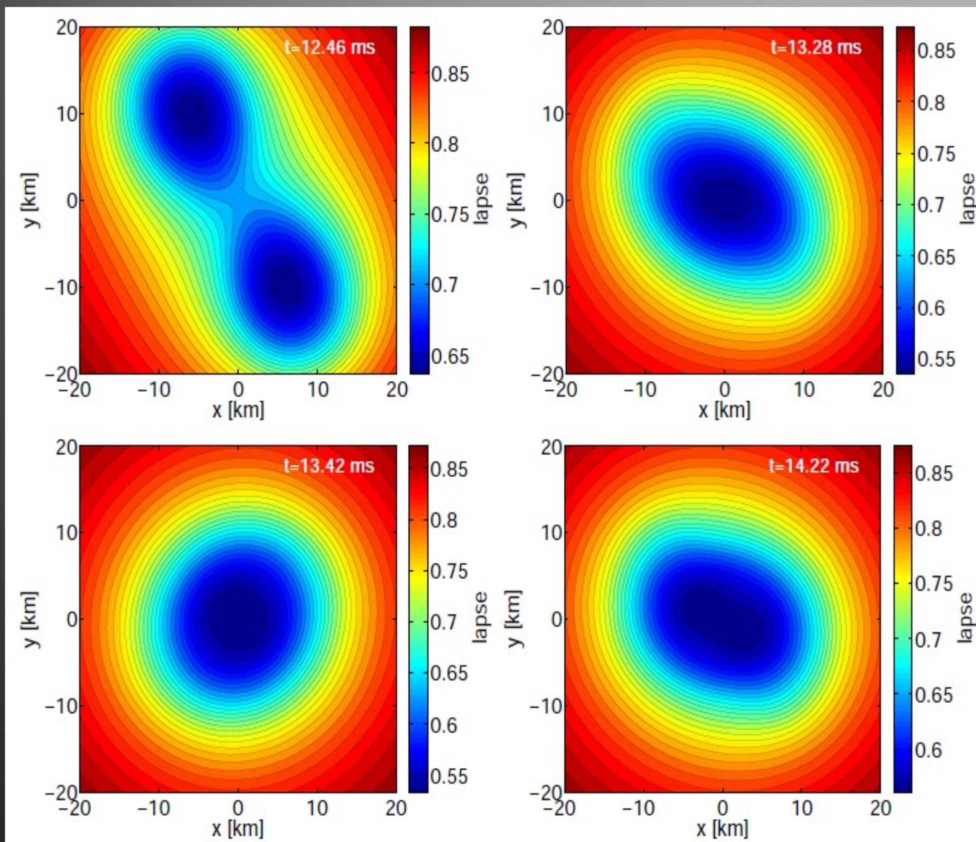

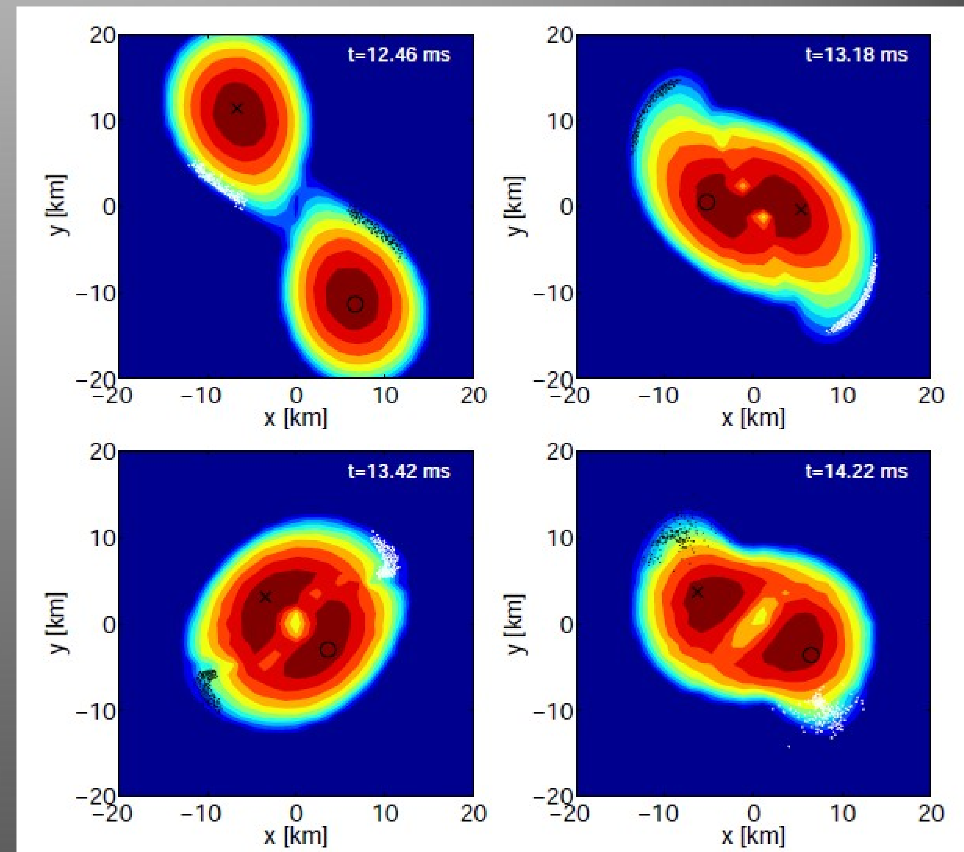

Bauswein et al. 2016

Same time steps: double cores are local overdensities of **single** isolated, selfgravitating object

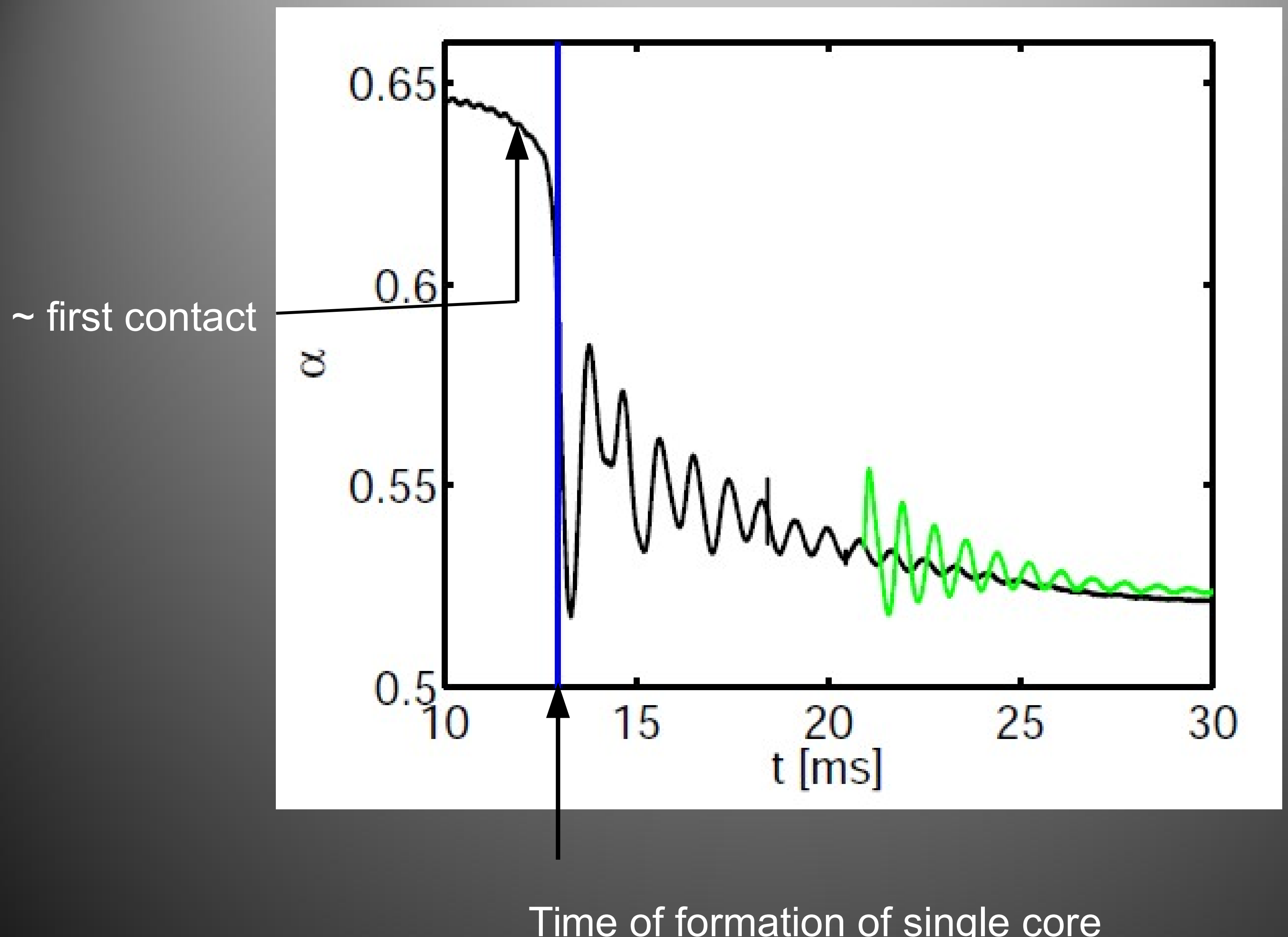

Evolution of central lapse, DD2 1.35-1.35 M_{sun}

Secondary GW features
in the postmerger spectrum

Generic GW spectrum

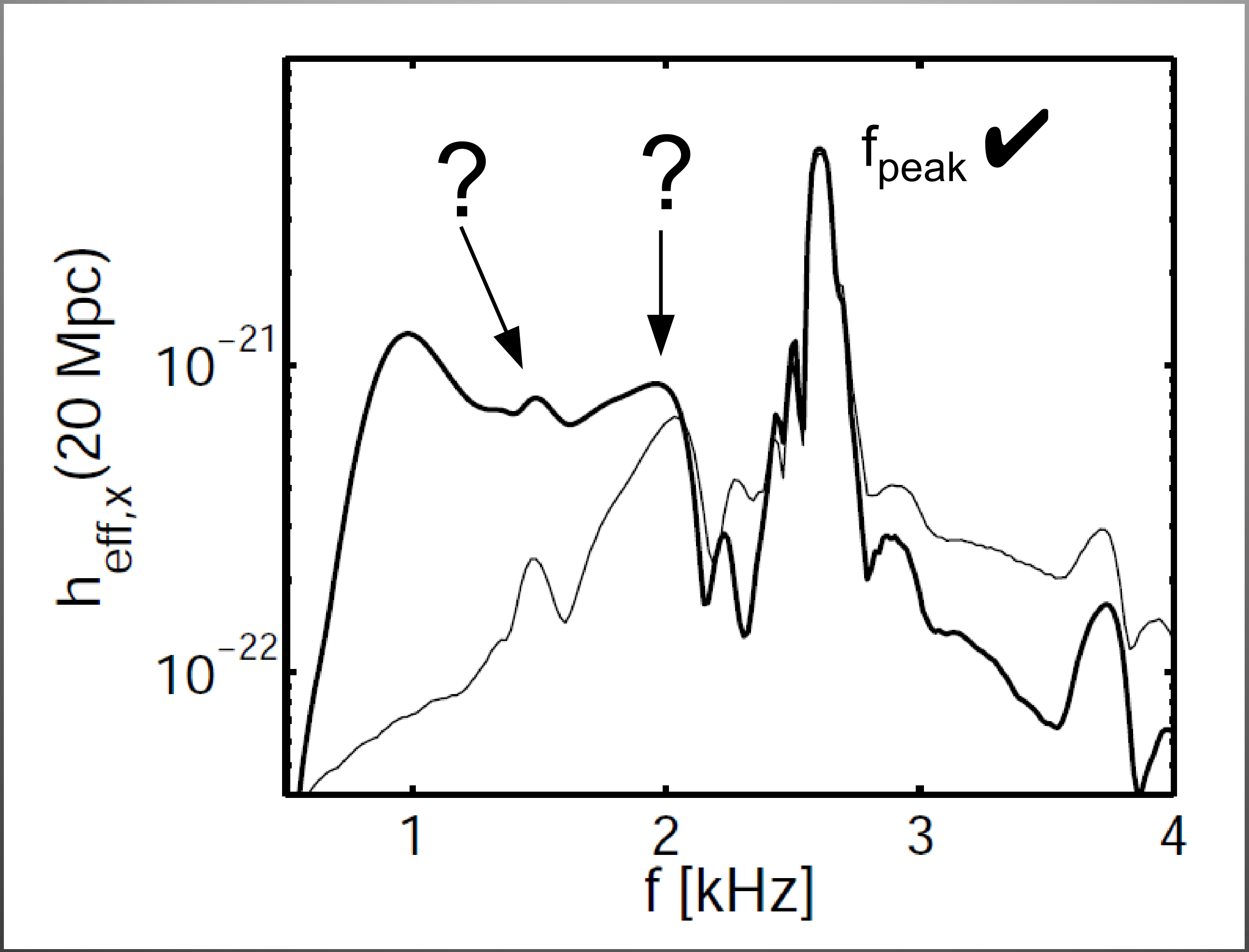

- Up to three pronounced features in the postmerger spectrum (+ structure at higher frequencies)
- 1.35-1.35 Msun DD2 EoS

Quasi-radial mode

- Central lapse function shows two frequencies (~500 Hz and ~1100 Hz)
- Add quasi-radial perturbation → re-excite quasi-radial mode
  => f_0 = 1100 Hz
- Confirmed by mode analysis → radial eigen function at f_0

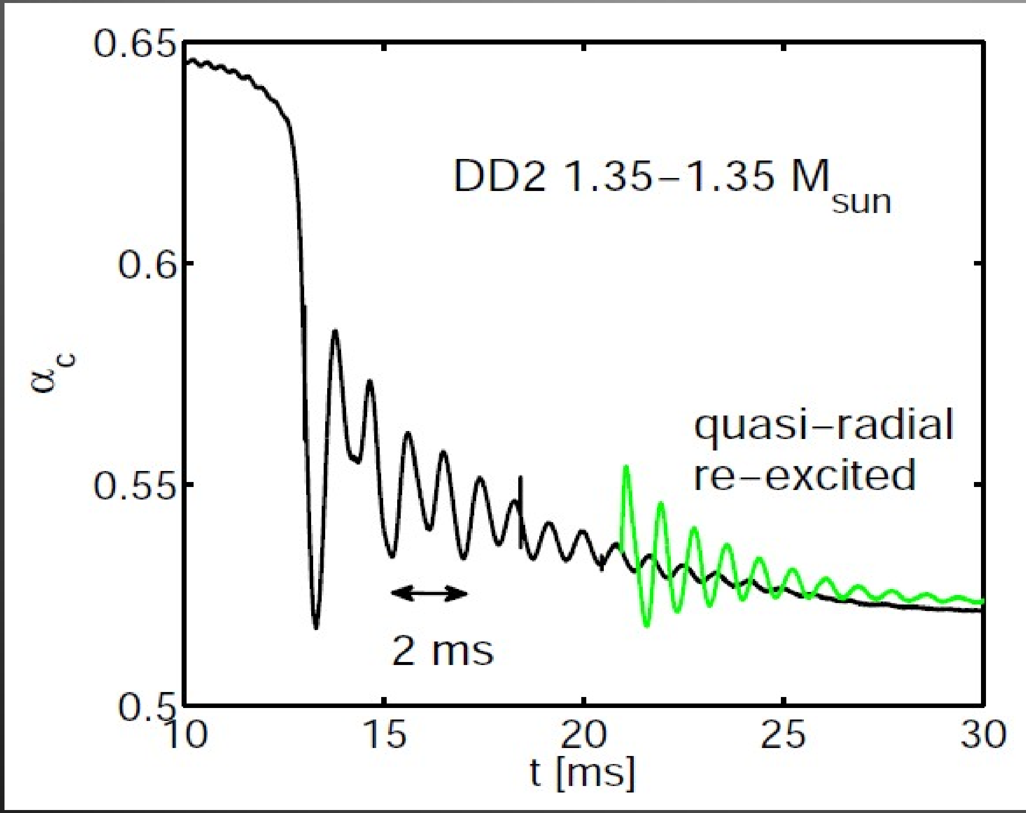

Bauswein et al. 2015

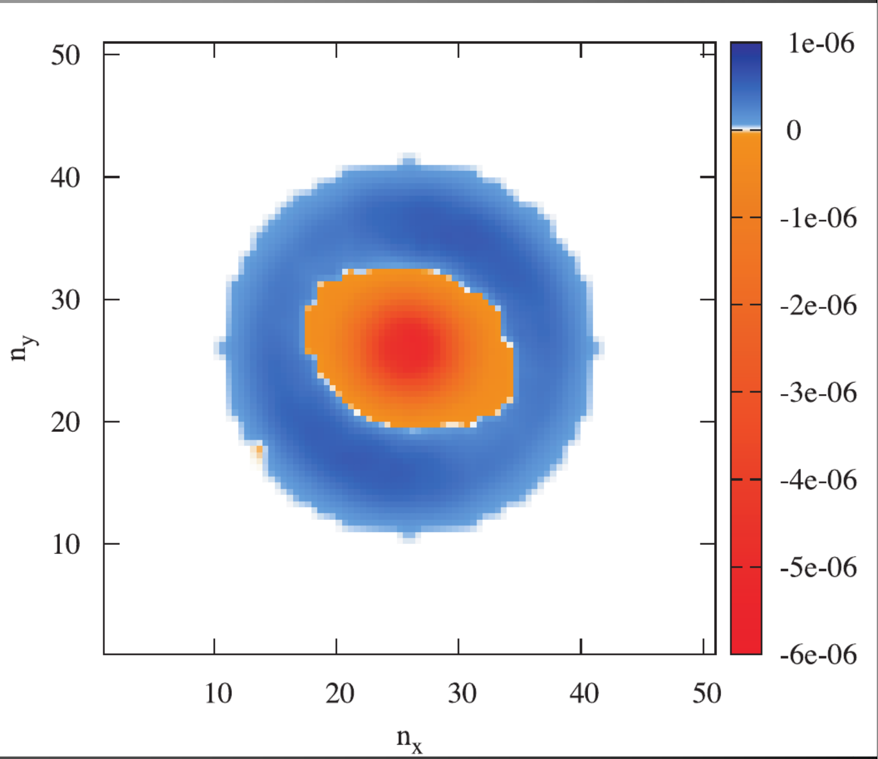

Stergioulas et al. 2011

Could consider also size of the remnant, rhomax, …

Note: additional low-frequency oscillation (500 Hz) also in GW amplitude (explained later)

Generic GW spectrum

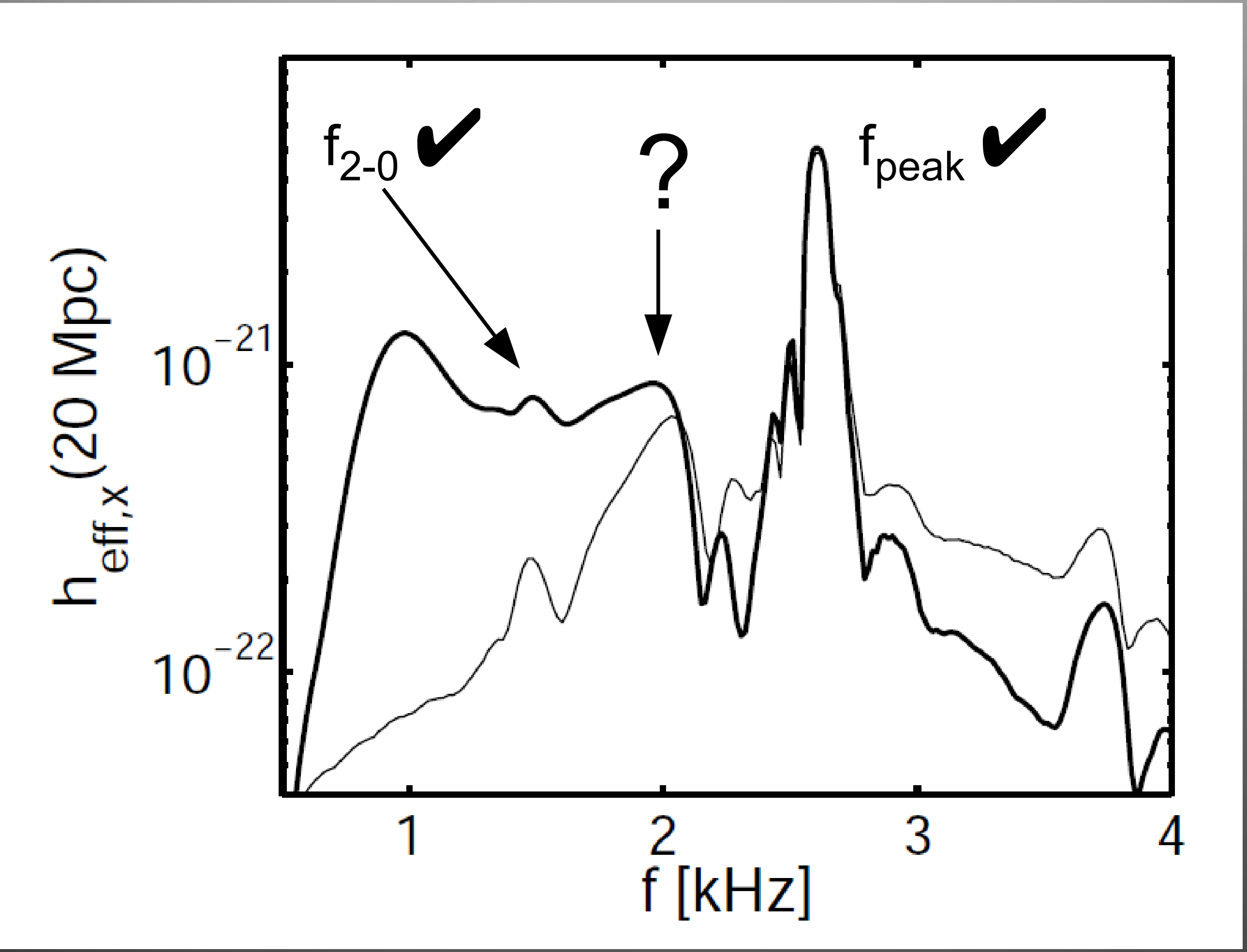

- Interaction between dominant quadrupolar mode and quasi-radial oscillation produced peak at $f_{2\text{-}0} = f_{peak} - f_0$ (see Stergioulas et al. 2011)

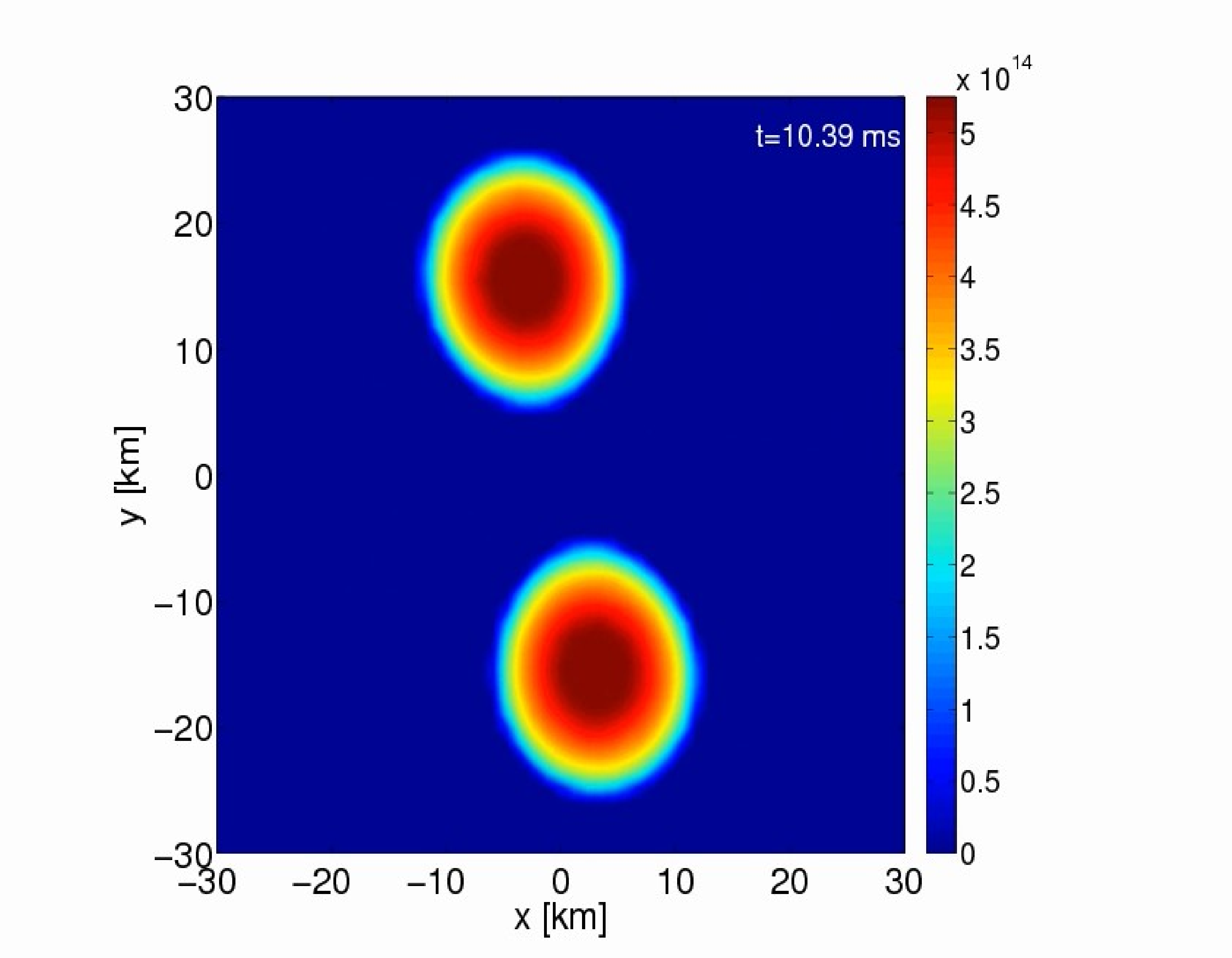

DD2 1.35-1.35 Msun, rest-mass density in the equatorial plane

Antipodal bulges (spiral pattern)

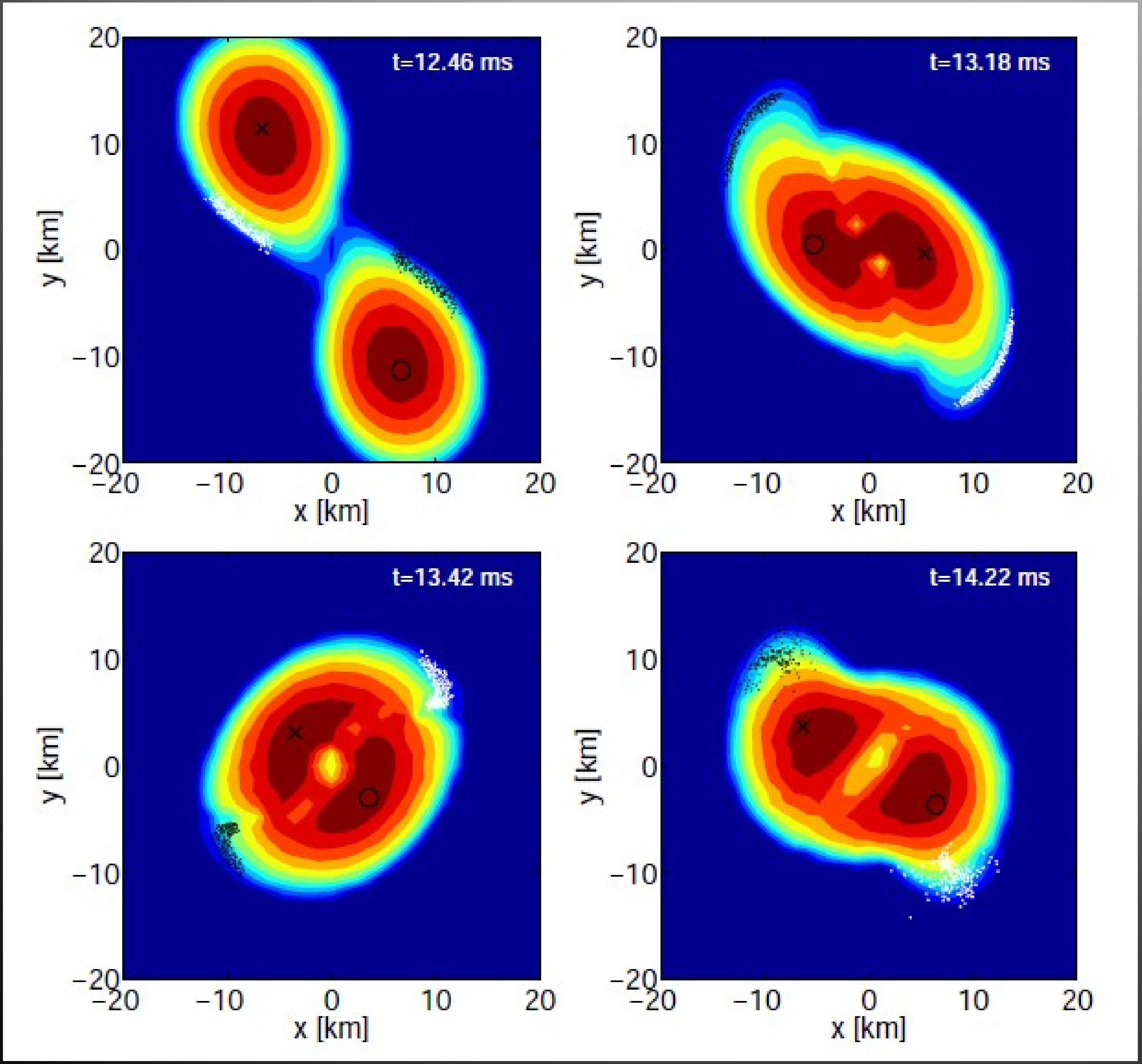

Bauswein et al. 2015

Orbital motion of antipodal bulges slower than inner part of the remnant (double-core structure)

Spiral pattern, created during merging lacks behind

Orbital frequency: 1/1ms → generates GW at 2 kHz !!!

Present for only a few ms / cycles

Generic GW spectrum

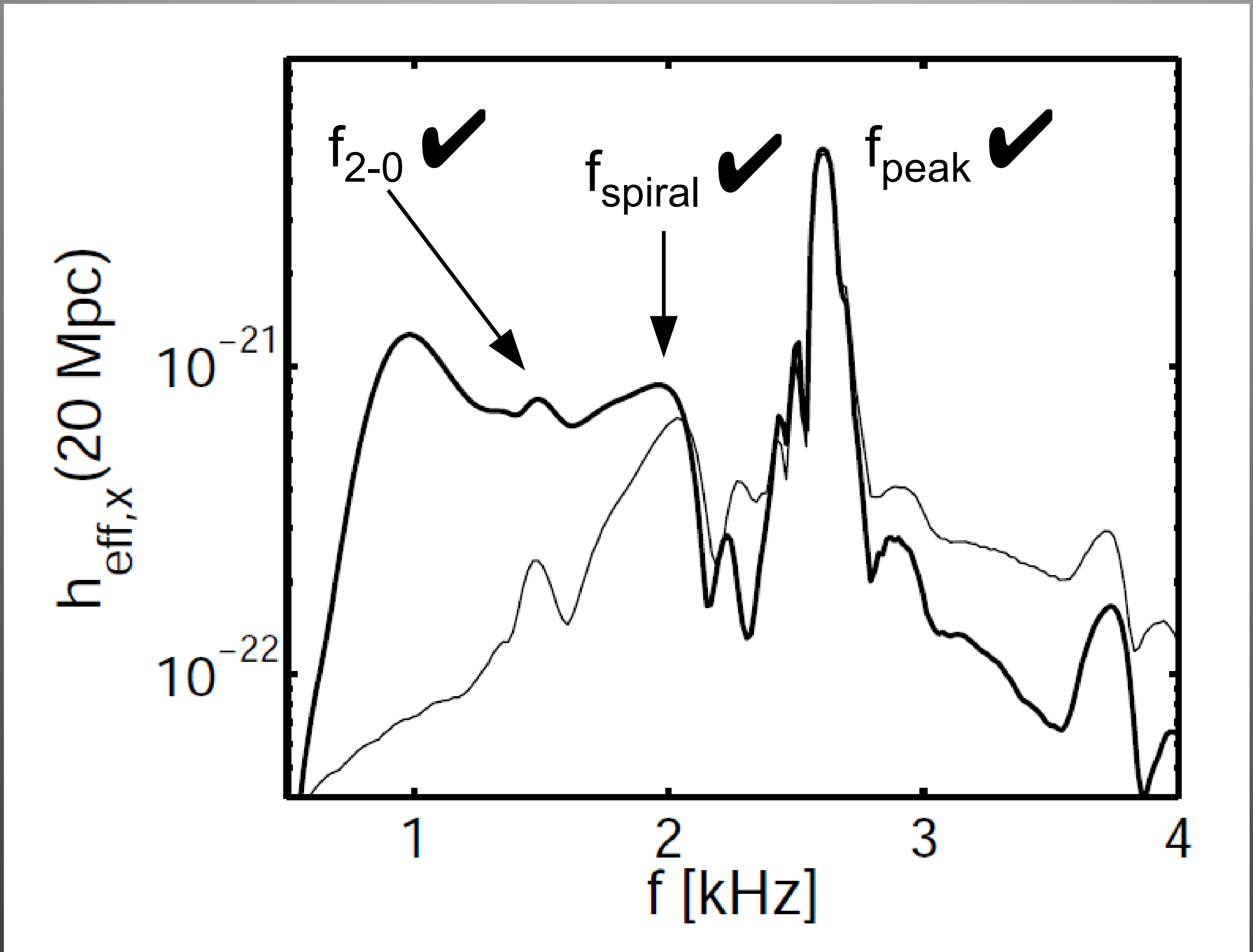

- Orbital motion of antipodal bulges generate peak at f_{spiral}

Further evidence

- Presence of spiral pattern coincides with presence of peak in GW spectrum
- Mass of bulges (several 0.1 M_{sun}) can explain strength of the peak by toy model of point particles the central remnant for a few ms
- Tracing dynamics / GW emission by computing spectra for “outer” and “inner” remnant → f_{spiral} emission is produced outside
- (Dynamics of double cores (inner remnant) fail to explain this emission)
- Spectrogram agrees with this picture (length, frequency), no strong time-variation of the dominant frequency

=> orbital motion => f_{spiral} peak

Example: TM1 1.35-1.35 Msun, strong tidal bulges, weak radial oscillation (e.g. from analysis of lapse)

Clark et al. 2016

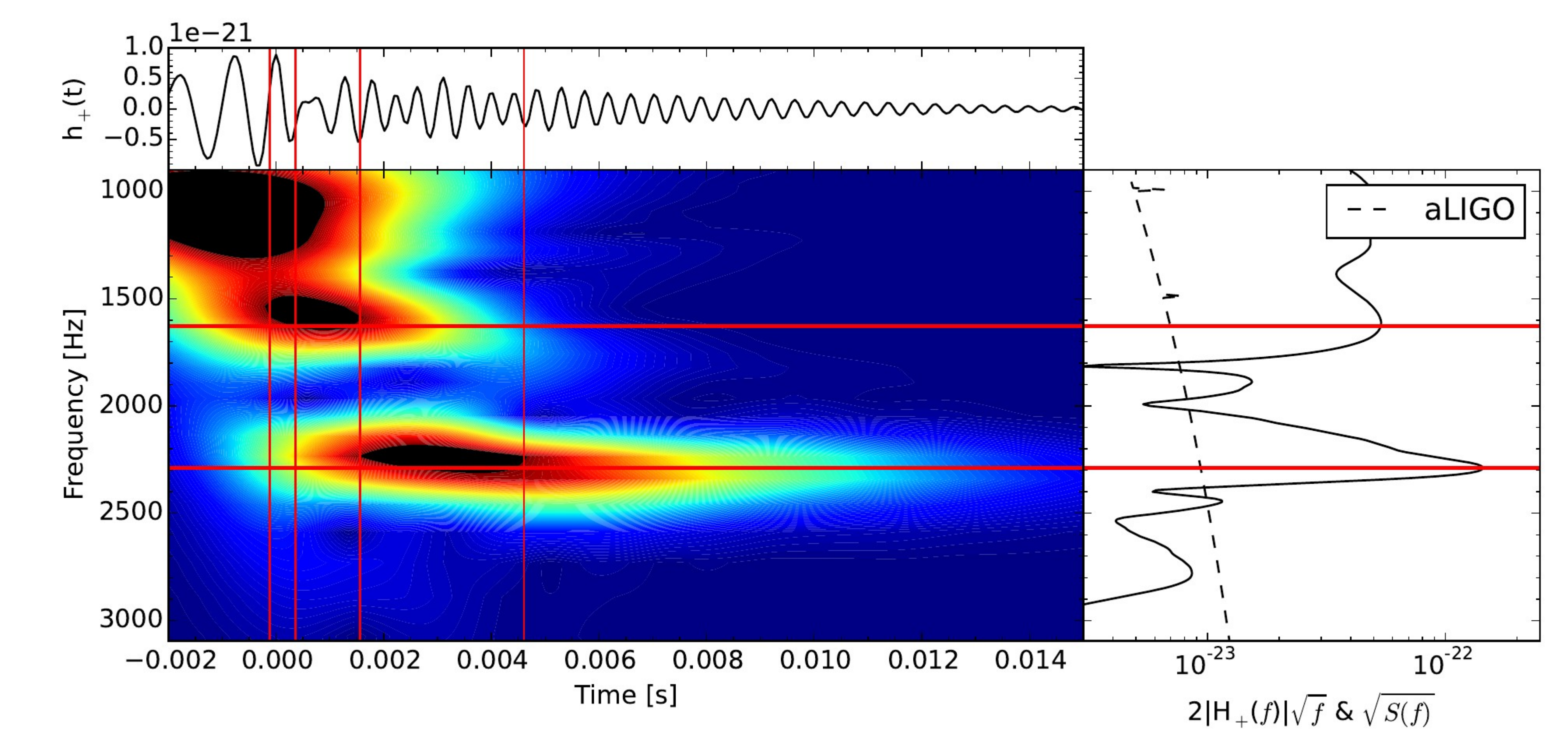

Note: different ideas about the origin of the peaks, e.g. Kastaun & Galeazzi 2015, Takami et al. 2014, 2015 propose a strongly varying instantaneous frequency that produces side peaks

Classification of postmerger GW spectra and dynamics

Survey of GW spectra

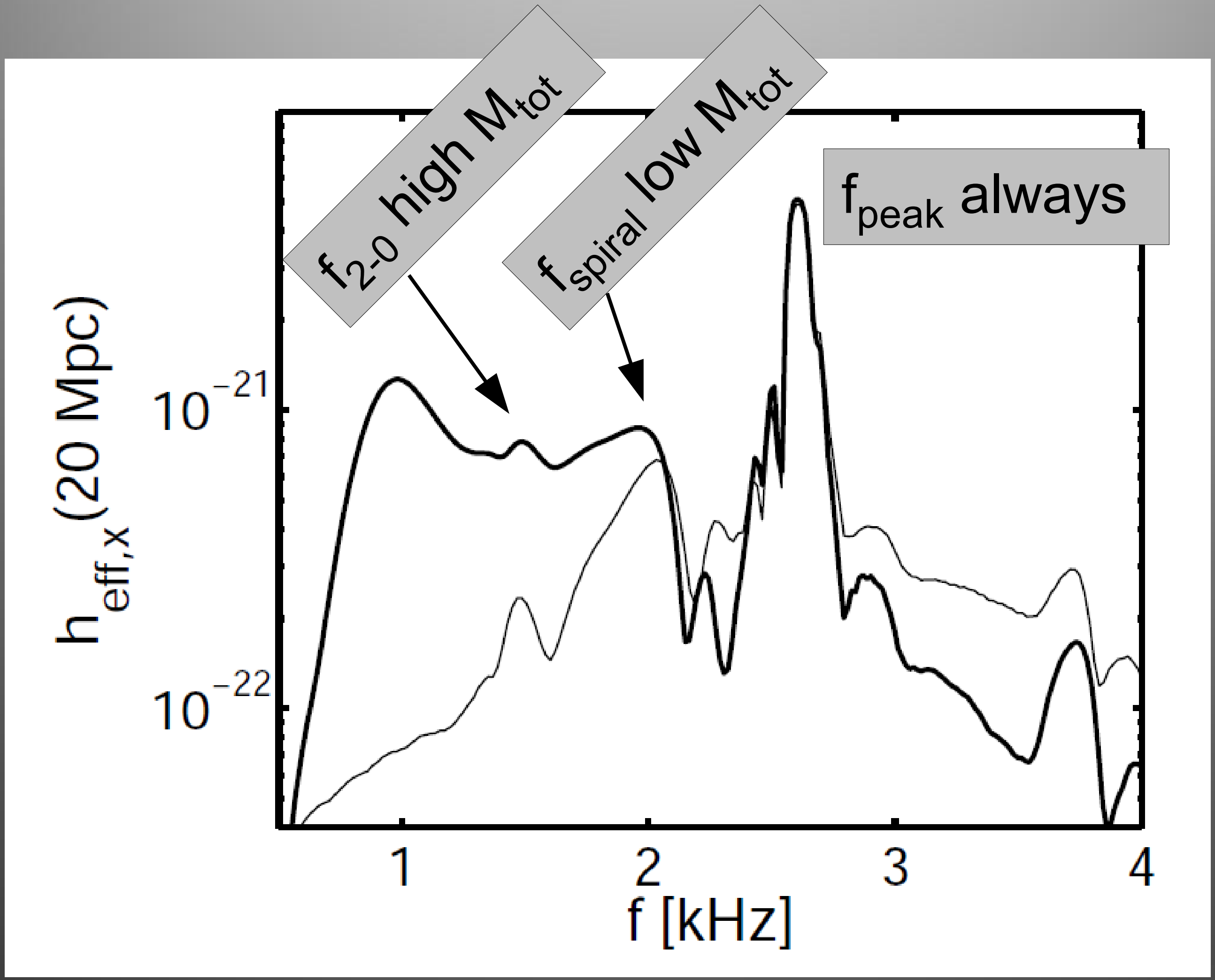

- Considering different models (EoS, M_{tot}): 3 types of spectra depending on presence of secondary features (dominant f_{peak} is always present)

Survey of GW spectra

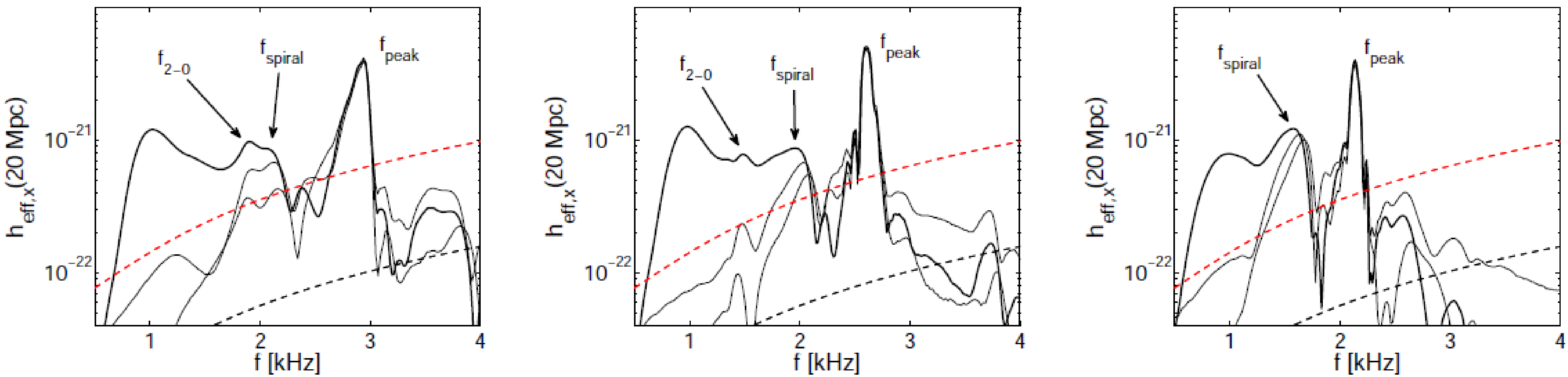

Type I Type II Type III

LS220, DD2, NL3 EoS all with M_{tot} = 2.7 M_{sun} → consider M_{tot} relative M_{thres}

Classification scheme

- Type I: 2-0 feature dominates, f_{spiral} hardly visible, radial mode strongly excited, observed for relatively high M_{tot}
- Type II: both secondary features have comparable strength, clearly distinguishable, moderate binary masses
- Type III: f_{spiral} dominates, f_{2-0} hardly visible, found for relatively low binary masses, (central lapse, GW amplitude, rhomax show low-frequency modulation in addition to radial oscillation)

- Different types show also different dynamical behavior, e.g. in central lapse, rhomax, ….
- High mass / low mass relative to threshold binary mass for prompt BH collapse (→ EoS dependent)
- Continuous transition between different types

=> Depending on binary model (EoS, M1/2) either one or the other or both features are present / dominant (if you measure a secondary peak you should always think whether it is f_{2-0} or f_{spiral})

Classification scheme

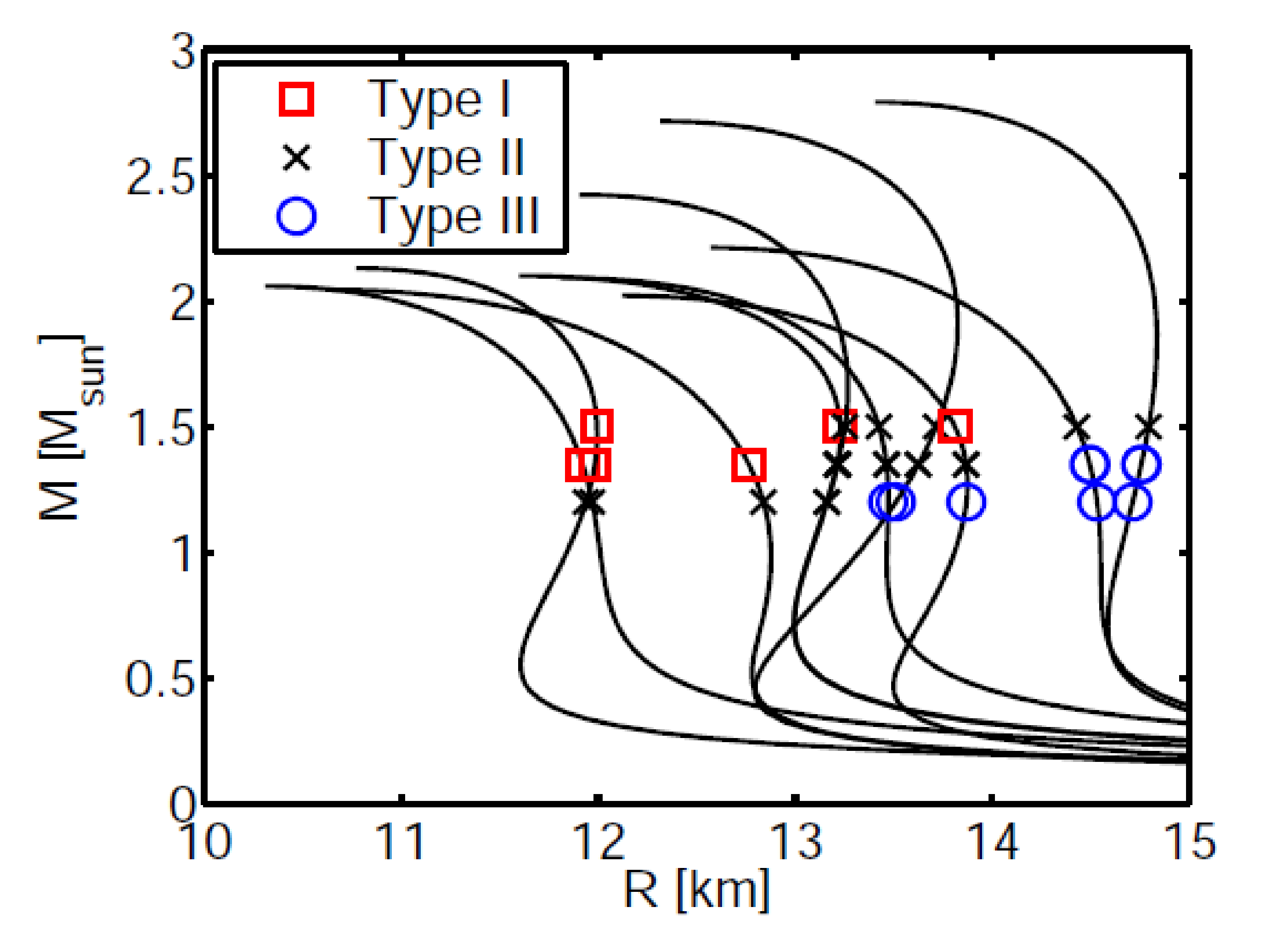

Bauswein et al. 2015

Type of M_1-M_2 merger indicate at $M_{tot}/2 = M_1$

(Continuous transition between types → tentative association)

For M_{tot} = 2.7 M_{sun} all Types are possible depending on EoS

Classification scheme

Behavior reasonable:

- Type I: compact NSs merge → high impact velocity / violent collision => radial oscillation strongly excited (2-0 dominant); higher compactness → formation of tidal bulges suppressed (f_{spiral} weaker)
- Type III: less compact NSs merge → lower impact velocity / smooth merging => radial mode suppressed (no 2-0); pronounced tidal bulges (strong f_{spiral} feature)

For Type III and Type II low-frequency modulation with $f_{low} = f_{peak} - f_{spiral}$ by orientation of bulge w. r. t. inner double-core/bar

(seen in lapse, GW amp., rhomax, ...)

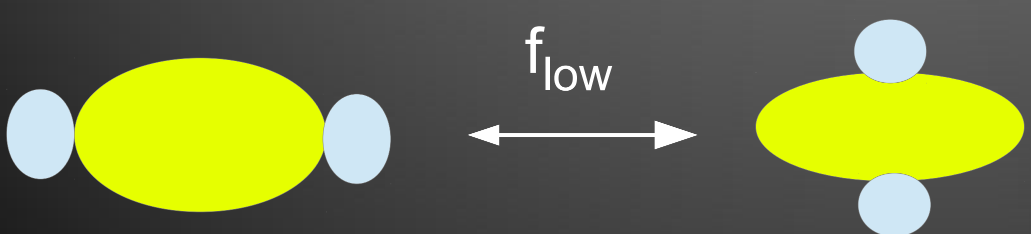

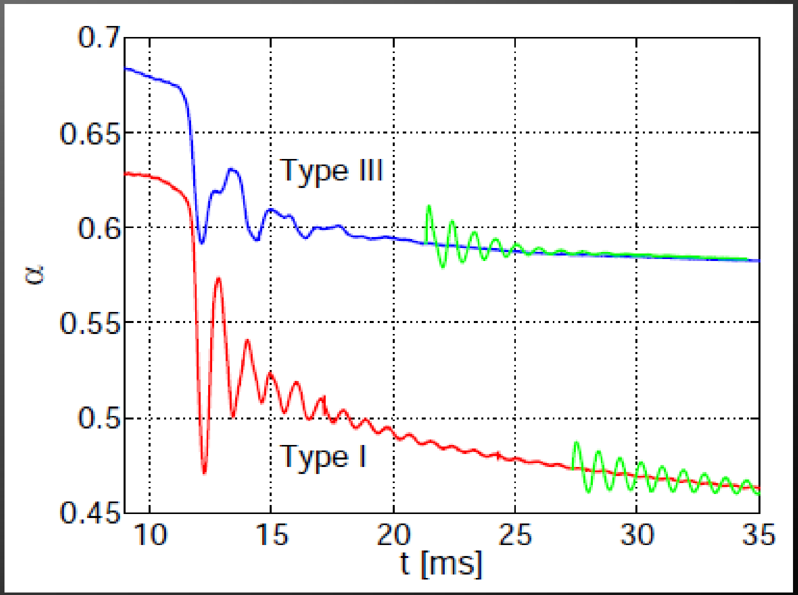

Dependencies of frequencies

Gravitational waves – EoS survey

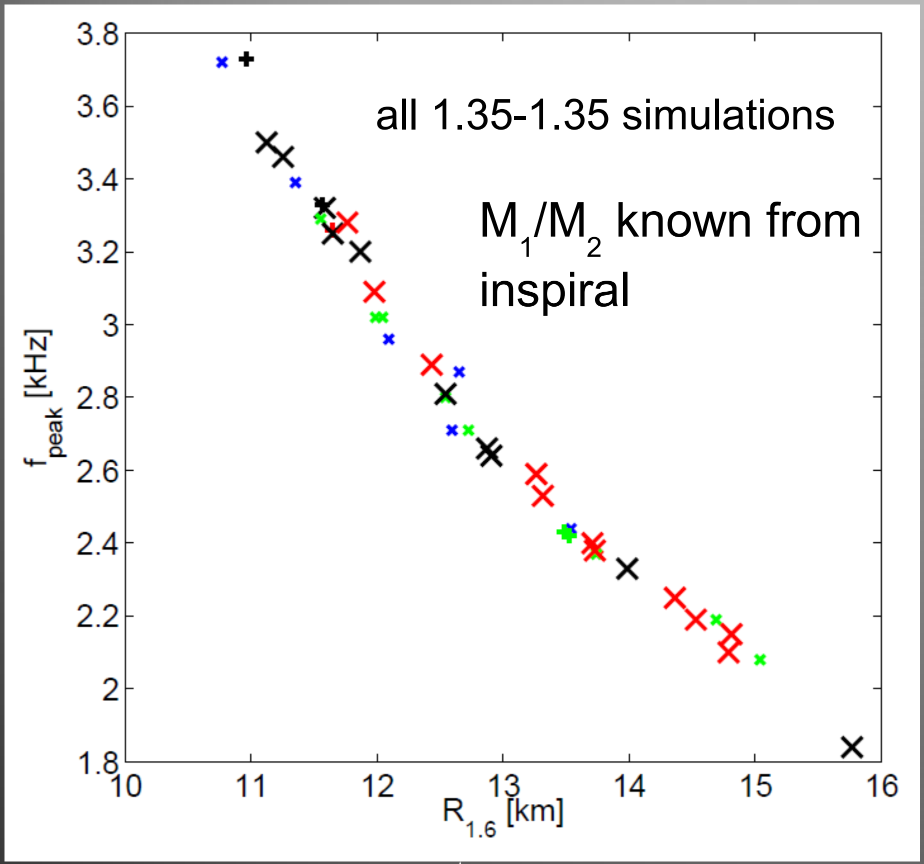

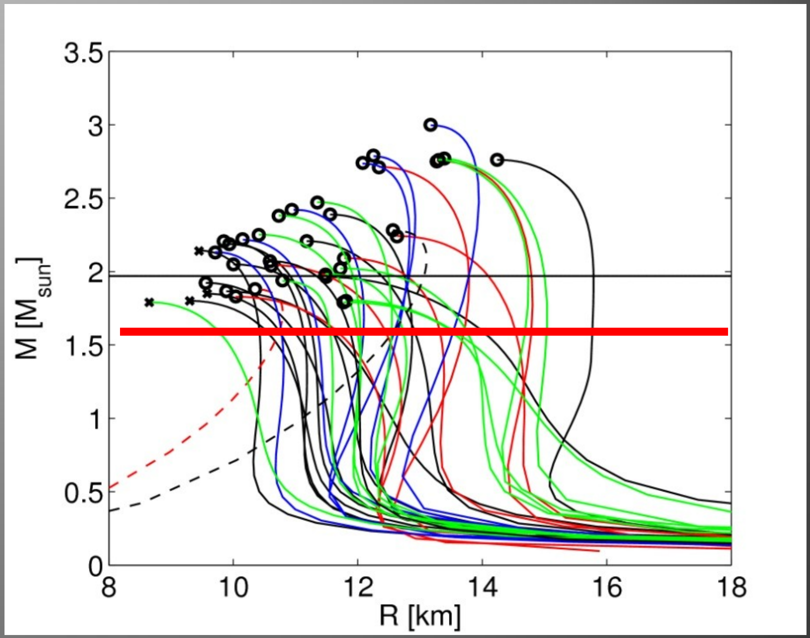

characterize EoS by radius of nonrotating NS with 1.6 M_{sun}

Bauswein et al. 2012

Pure TOV/EoS property => Radius measurement via f_{peak}

Important: Simulations for the same binary system, just with varied EoS

Note: R of 1.6 M_{sun} NS scales with f_{peak} from 1.35-1.35 M_{sun} mergers (density regimes comparable)

Binary mass variations

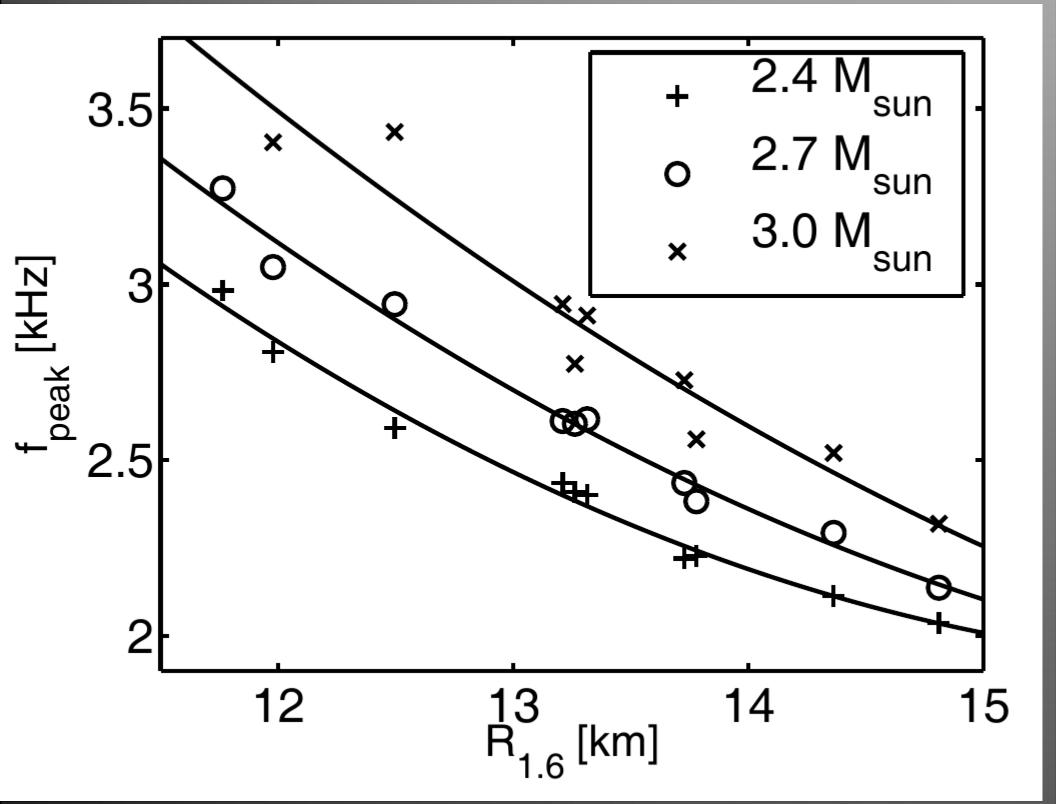

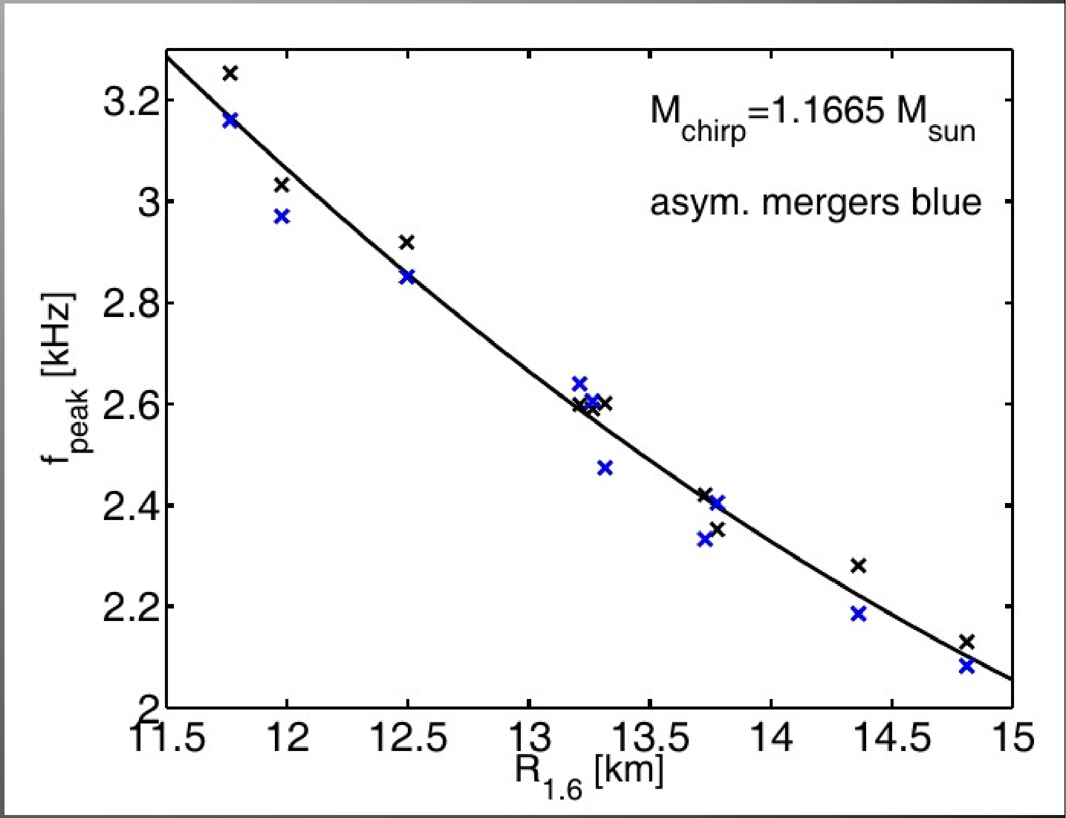

Different total binary masses (symmetric)

Fixed chirp mass (incl. Asymmertic binaries)

Bauswein et al. 2016

Dependencies of secondary frequencies

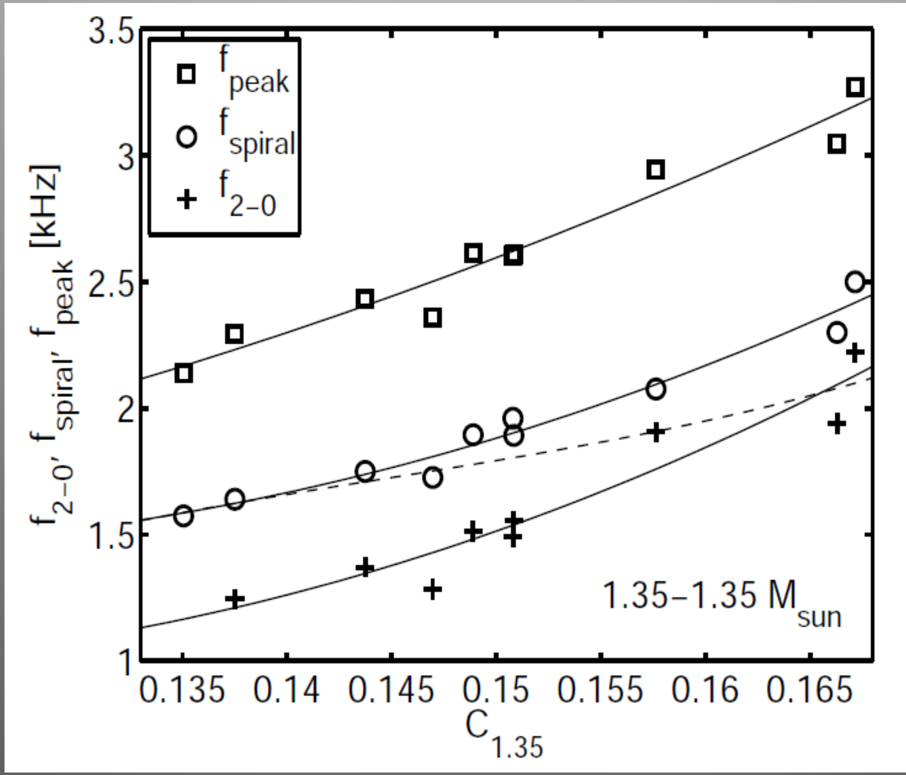

For fixed M_{tot} = 2.7 M_{sun}

Dashed line from Takami et al. 2014

Bauswein et al. 2015

EoS characterized by compactness C=M/R of inspiralling stars (equivalent to radius as before)

All three frequencies scale similarly with compactness (equivalently radius since M = M_{tot}/2 = fixed here)

Here: only temperature-dependent EoS to avoid uncertainties/ambiguities due to approximate treatment of thermal effects (Gamma_th)

For small binary mass asymmetry only small quantitative shifts

Different binary masses

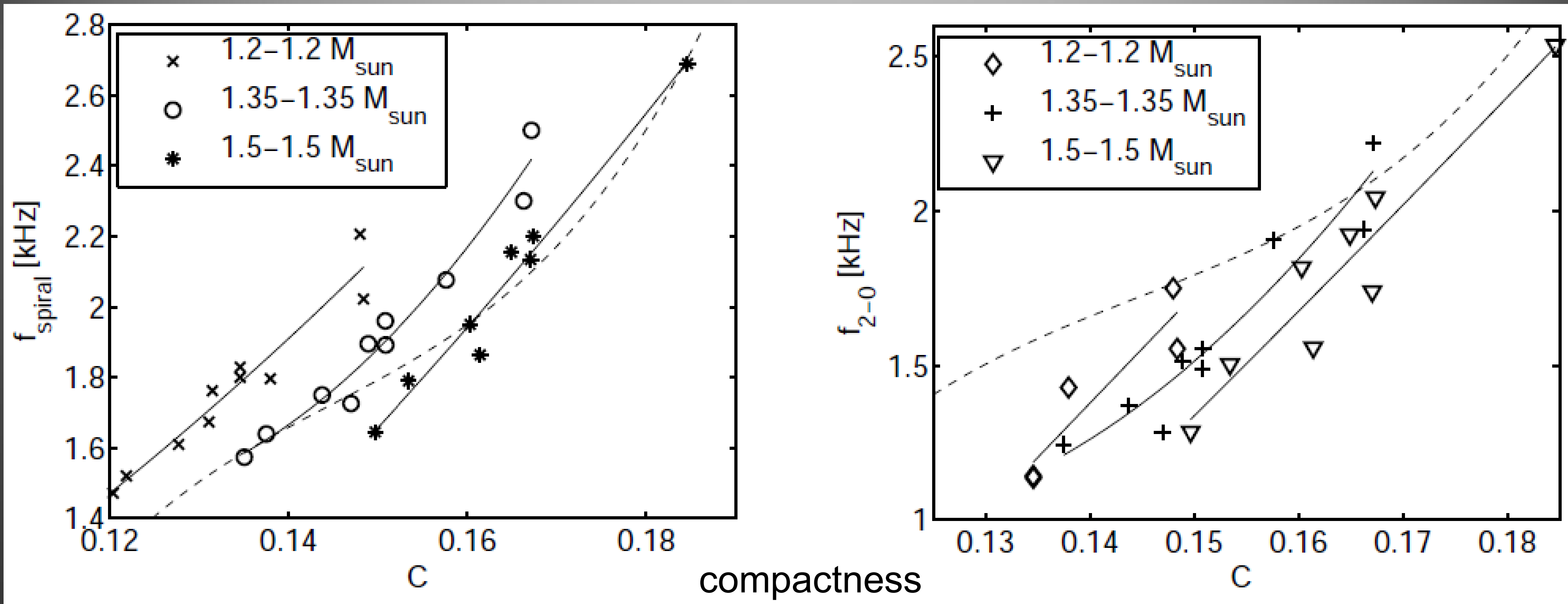

Bauswein et al. 2015

Dashed line from Takami et al. 2014

- for the individual secondary frequencies there are relations between C and the frequency for fixed binary masses (solid lines)
- (binary masses will be known from GW inspiral signal)
- there is no single, universal, mass-independent relation (for a expected range of binary masses), also when choosing the strongest secondary peak
- no conflict with Takami et al.'s data (frequencies agree when comparing same models), but here constant binary mass range for every EoS, more EoSs (larger, more representative parameter range (EoS, M_{tot}))

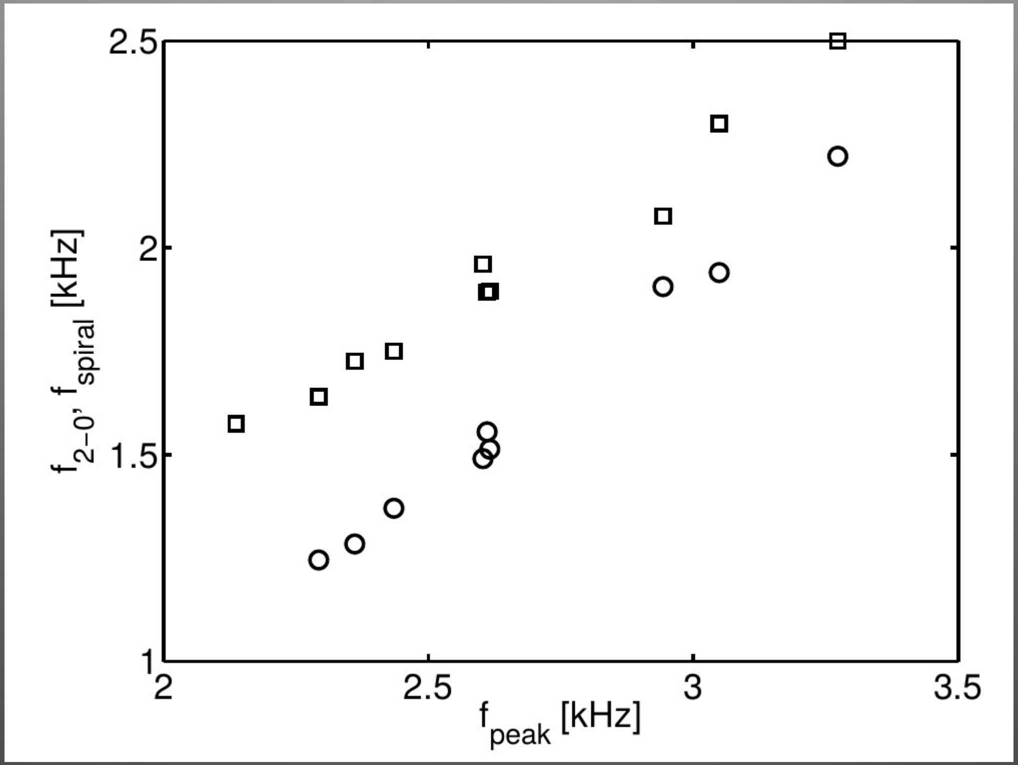

1.35-1.35 Msun

Clark et al. 2016

→ secondary frequencies are essentially given by dominant frequency

Universality of GW spectrum

Symmetric binary

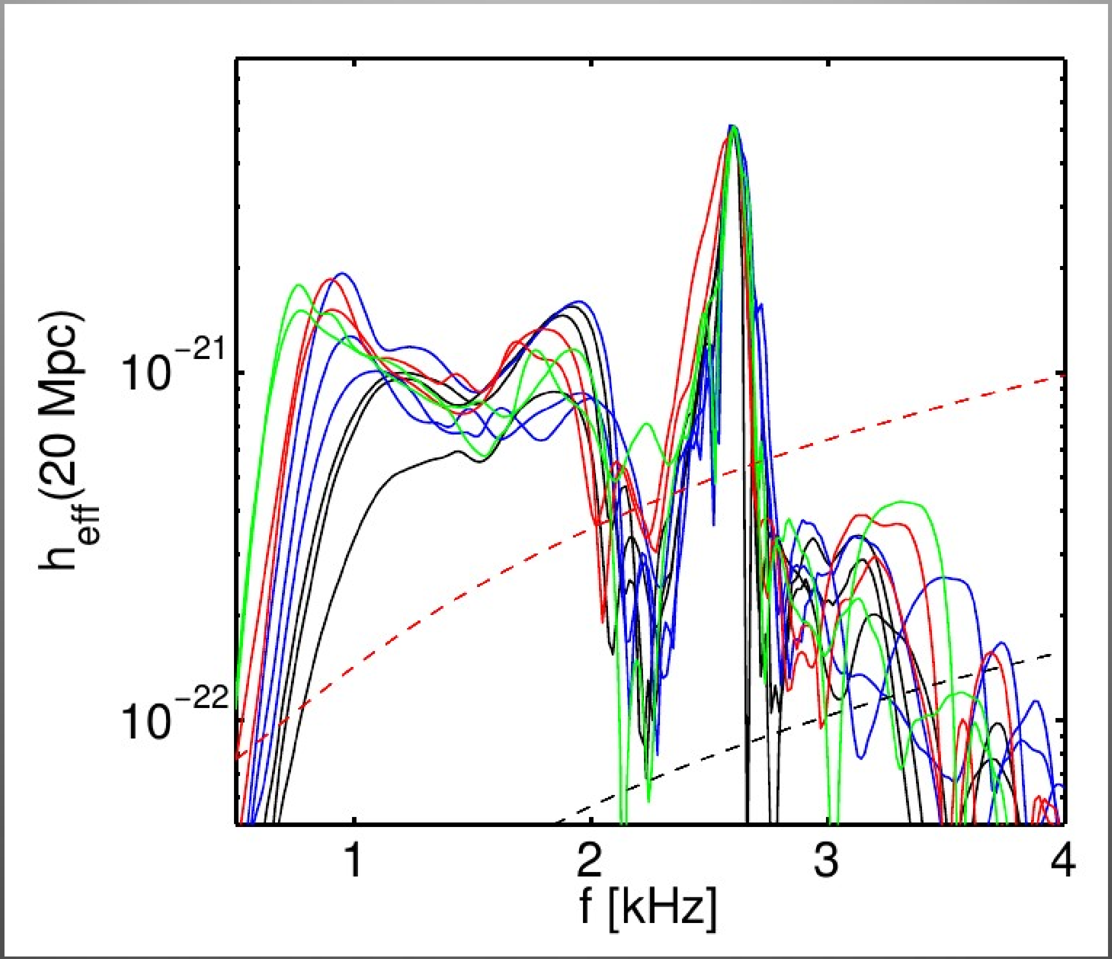

$a f_{\mathrm{sec}} = f_{\mathrm{ref}} f_{\mathrm{sec}} / f_{\mathrm{peak}}$

Bauswein et al. 2015

Rescaled to reference frequency f_{ref}=2.6 kHz with $a = f_{ref}/f_{peak}$

$$\Rightarrow a f_{sec} = f_{ref} f_{sec} / f_{peak} = f_{ref} \cdot const$$

→ universal spectrum basis of using PCA for GW data analysis

Principal Component Analysis

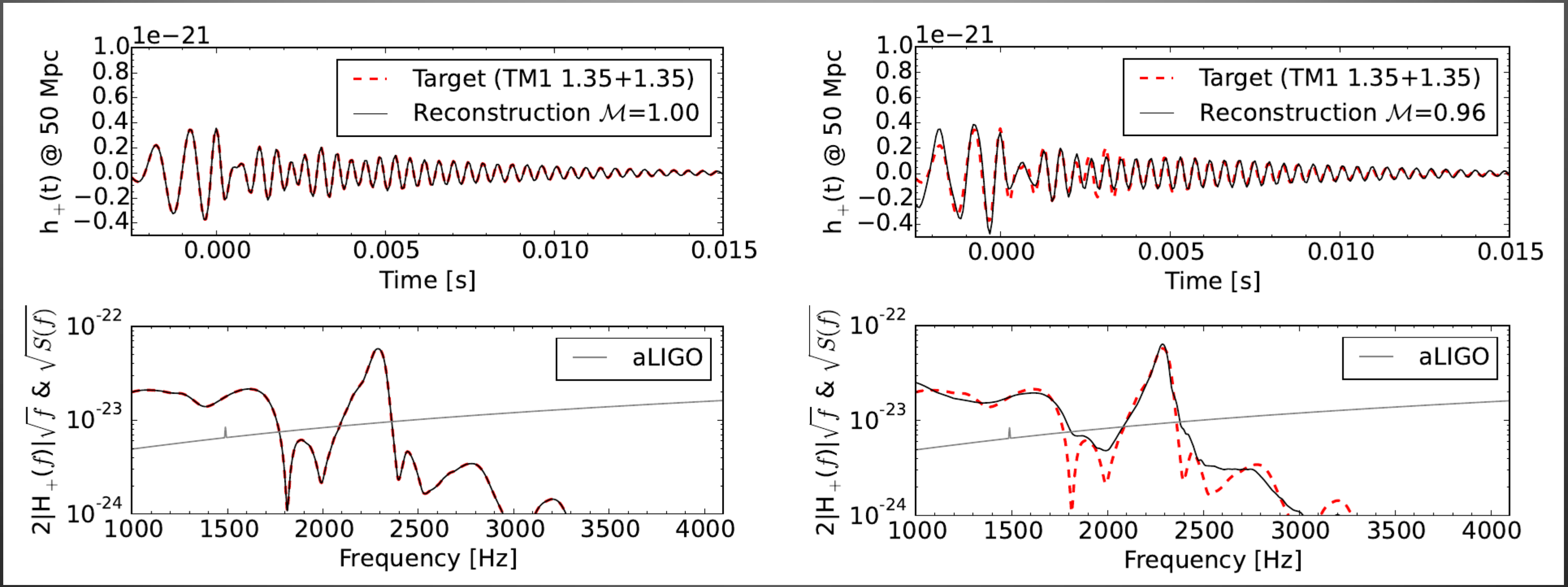

Only first component

Excluding the reconstructed waveform from catalogue

Clark et al 2016

Analytical model of postmerger GW emission

$$\begin{aligned} h_\times \propto Q_{xy} = & A_{\rm peak} \exp\left(-(t-t_0)/\tau_{\rm peak}\right) \\ & \sin\left(2\pi f_{\rm peak}(t-t_0)+\phi_{\rm peak}\right) \\ & +A_{\rm spiral} \exp\left(-(t-t_0)/\tau_{\rm spiral}\right) \\ & \sin\left(2\pi f_{\rm spiral}(t-t_0)+\phi_{\rm spiral}\right) \\ & +A_{2-0} \exp\left(-(t-t_0)/\tau_{2-0}\right) \\ & \sin(2\pi f_{2-0}(t-t_0)+\phi_{2-0}), \end{aligned}$$

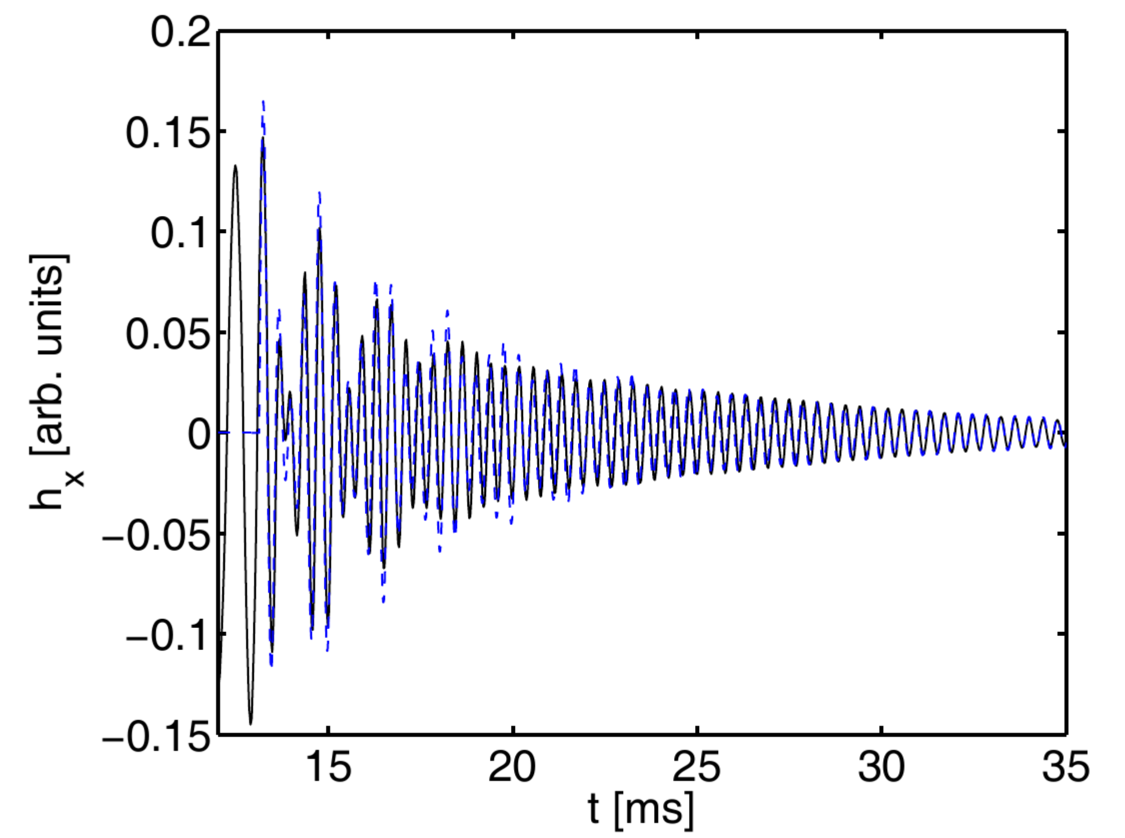

Parameter tuning only by eye !

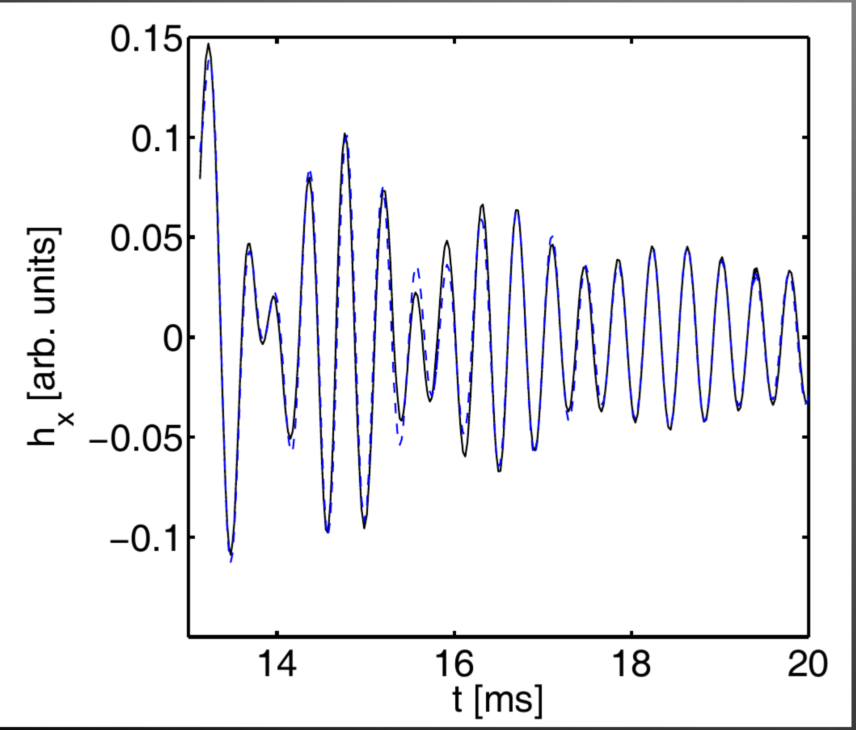

fit

Bauswein et al. 2016

Summary

- Certain features of postmerger remnant can be described as oscillation modes: f-mode, quasi-radial mode
- Secondary GW peak by tidal bulges
- Classification scheme of postmerger spectra depending on presence of secondary peaks: three different types (depending on mass)
- Dominant frequency scales tightly with NS radius → measurements
- Secondary frequencies scale with radii of non-rotating NSs for fixed total mass or with dominant frequency
- Universality of GW spectrum
- Analytic model of postmerger emission

Details: Bauswein & Stergioulas, PRD 91, 124056 (2015)
Bauswein, Stergioulas, Janka, EPJA 52, 56 (2016)

Impact of intrinsic rotation

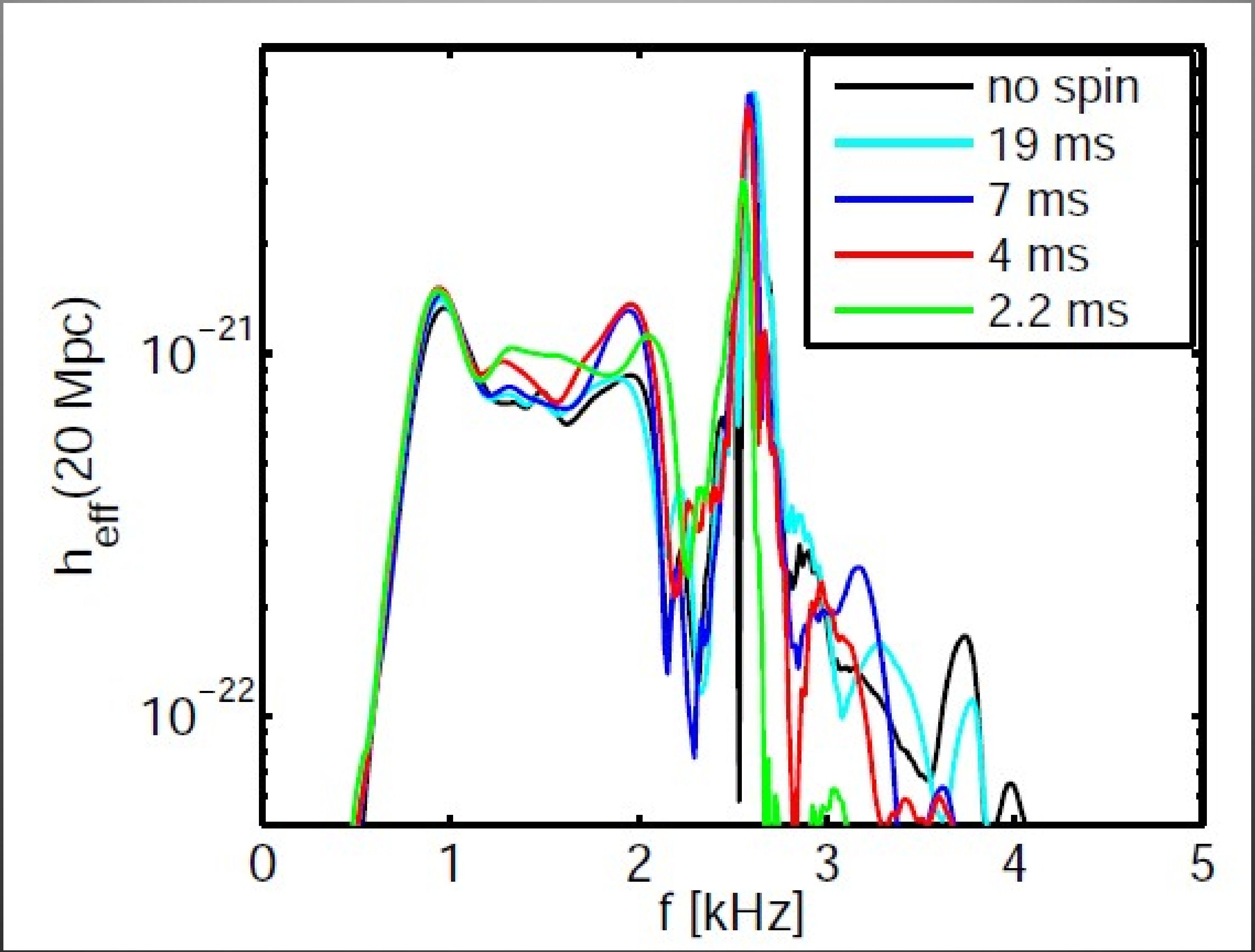

DD2 1.35-1.35 M_{sun} – fastest known pulsar in binary 22 ms !!

Interpretation

Frequency of the fundamental quadrupolar fluid mode:

$$f \propto \sqrt{\frac{M}{{R_{rem}}^3}}$$

(inverse dynamical timescale)

$$R_{rem} \propto R_{1.6}$$

$$\Rightarrow f_{peak} \propto {R_{1.6}}^{-3/2}$$

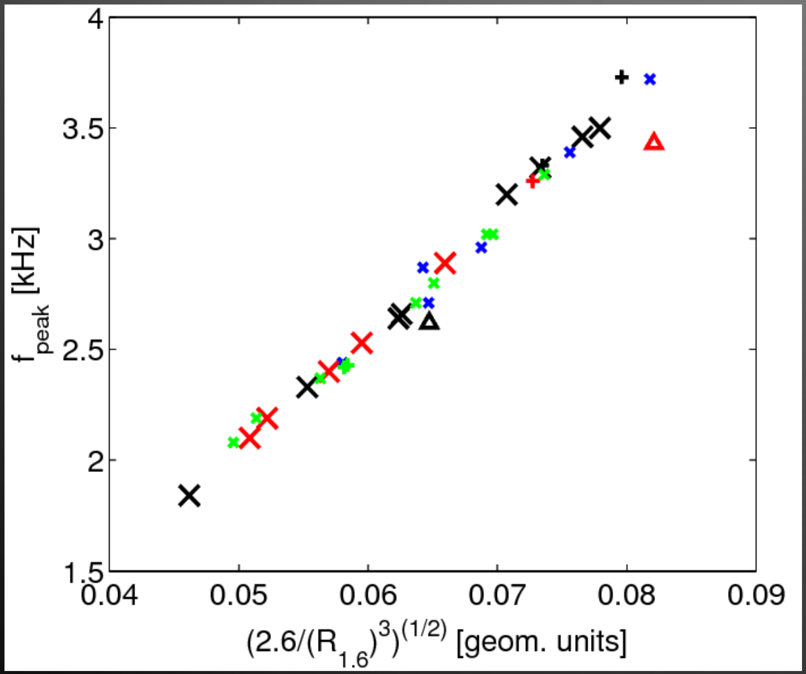

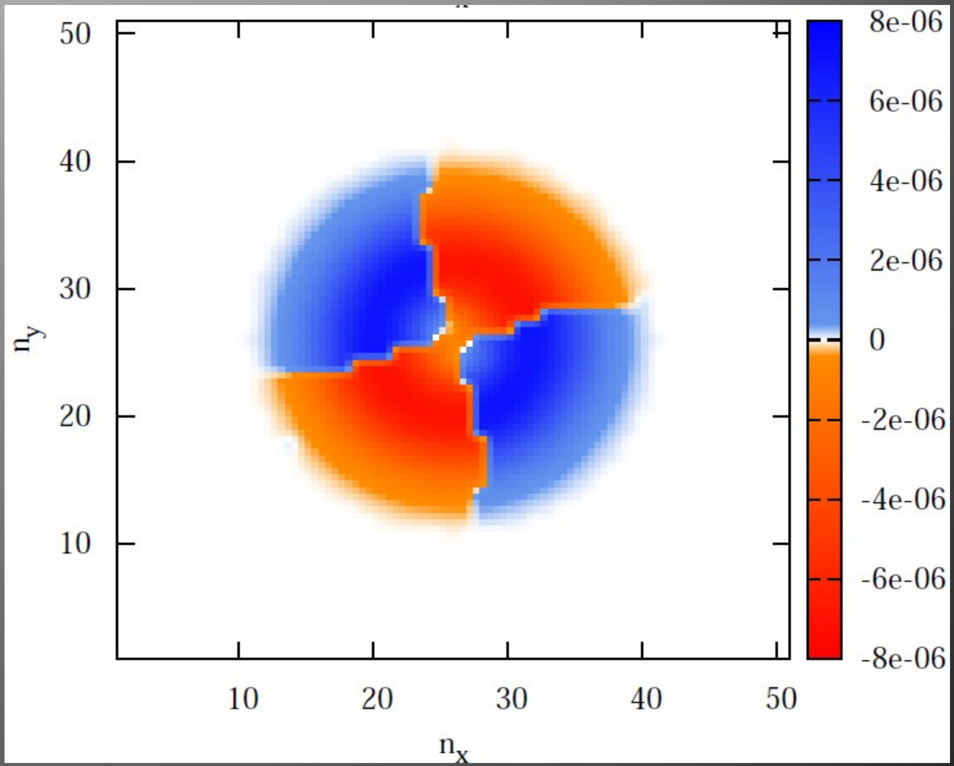

Mode analysis (Stergioulas et al. 2011)

Comparison

H4 1.3-1.3 Msun

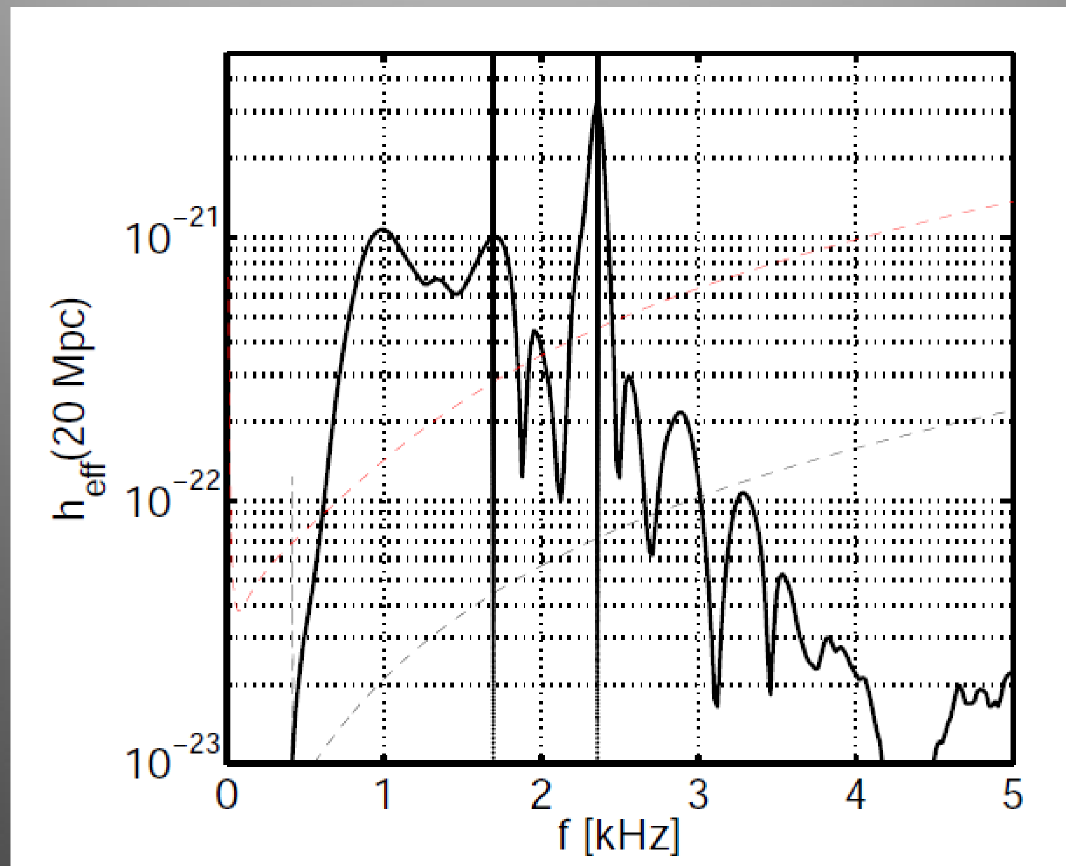

Binary	f_{max} [Hz]	f_1 [Hz]	f_2 [Hz]
H4-q10-M1275	1464	1645	2377
H4-q10-M1300	1489	1696	2356
H4-q10-M1325	1494	1702	2449

Takami et al. 2015

Strategy: Different binary masses

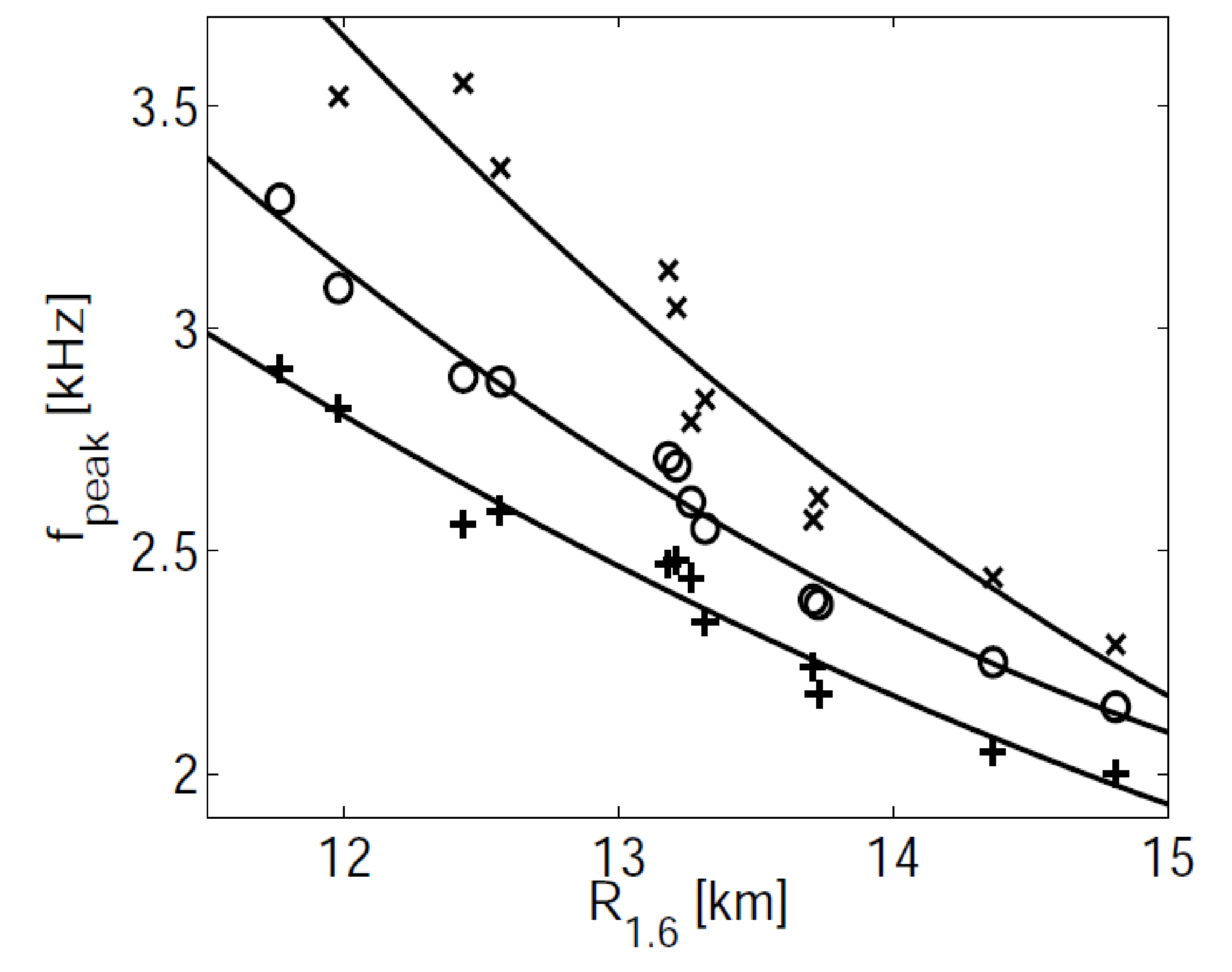

+ 1.2-1.2 M_{sun}

o 1.35-1.35 M_{sun}

x 1.5-1.5 M_{sun}

Maximum deviation determines error:

2.4 M_{sun}: 300 m
2.7 M_{sun}: 200 m
3.0 M_{sun}: 300 m

(can be further minimized)
(very similar relations for unequal masses)

Strategy: → Measure binary masses from inspiral GW signal
→ Choose relation depending on binary mass
→ Invert relation to obtain NS radius

Dependence on total binary mass

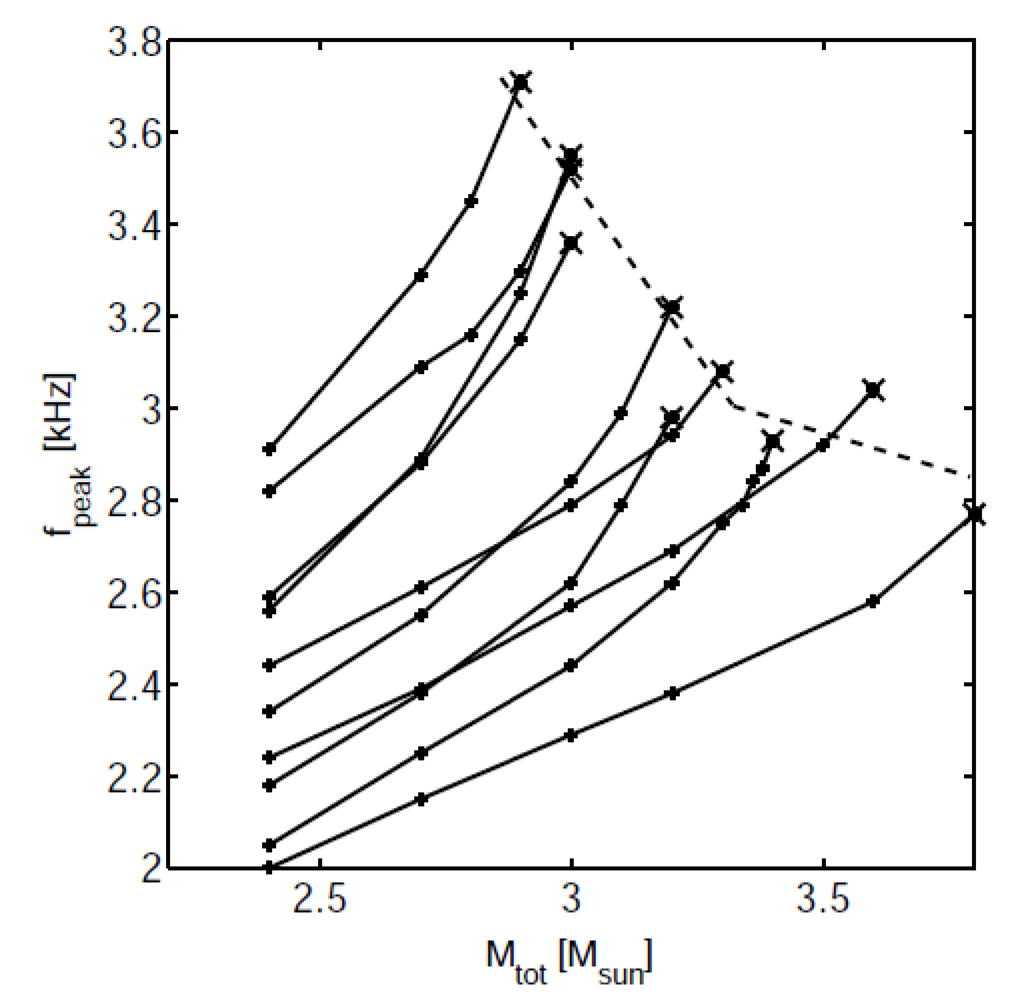

(every single line corresponds to a specific EoS
→ only one line can be the true EoS)

Dominant GW frequency monotone function of M_{tot}

Threshold to prompt BH collapse shows a clear dependence on M_{tot} (dashed line)

Threshold to prompt BH collapse

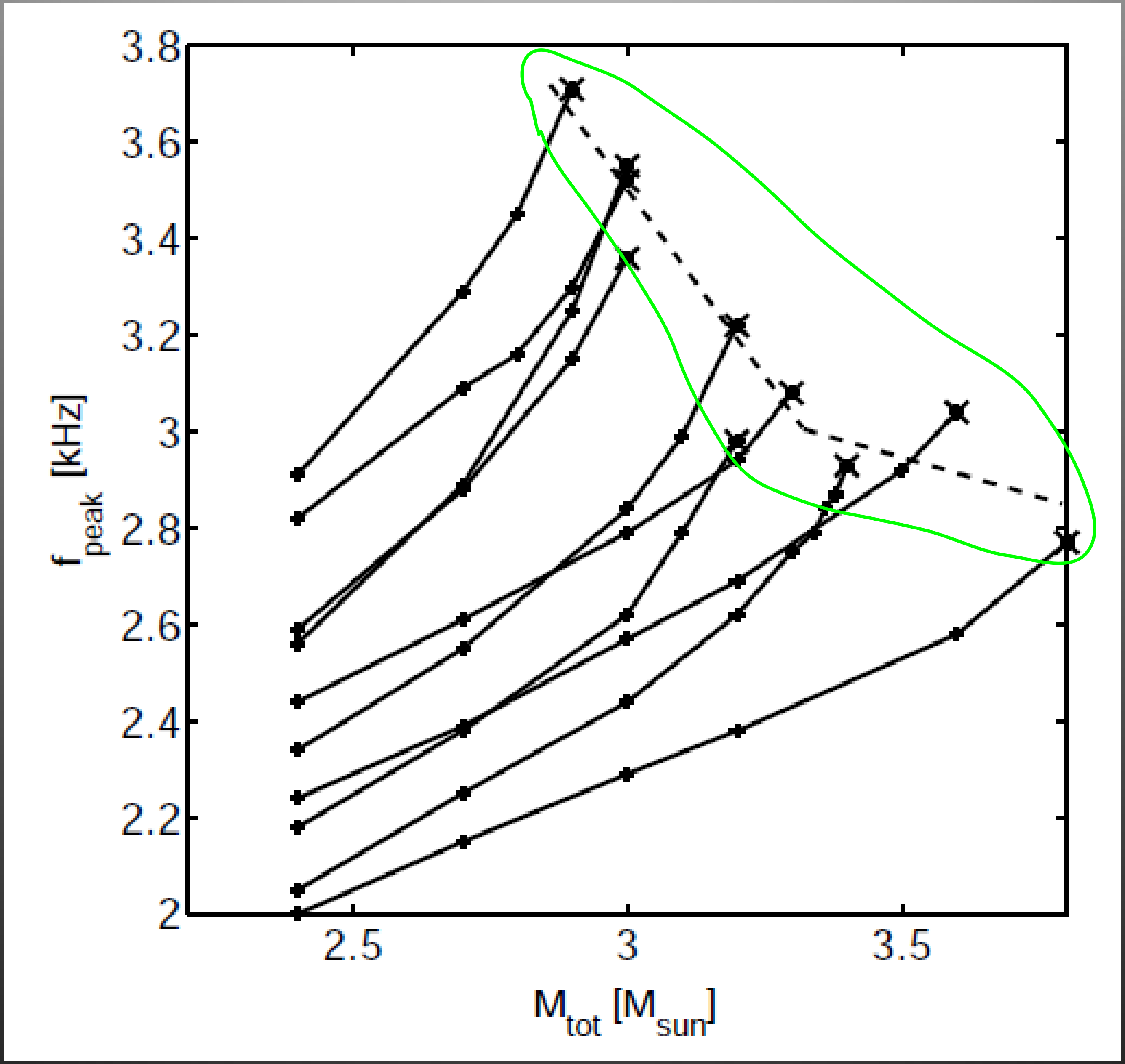

Extrapolation procedure

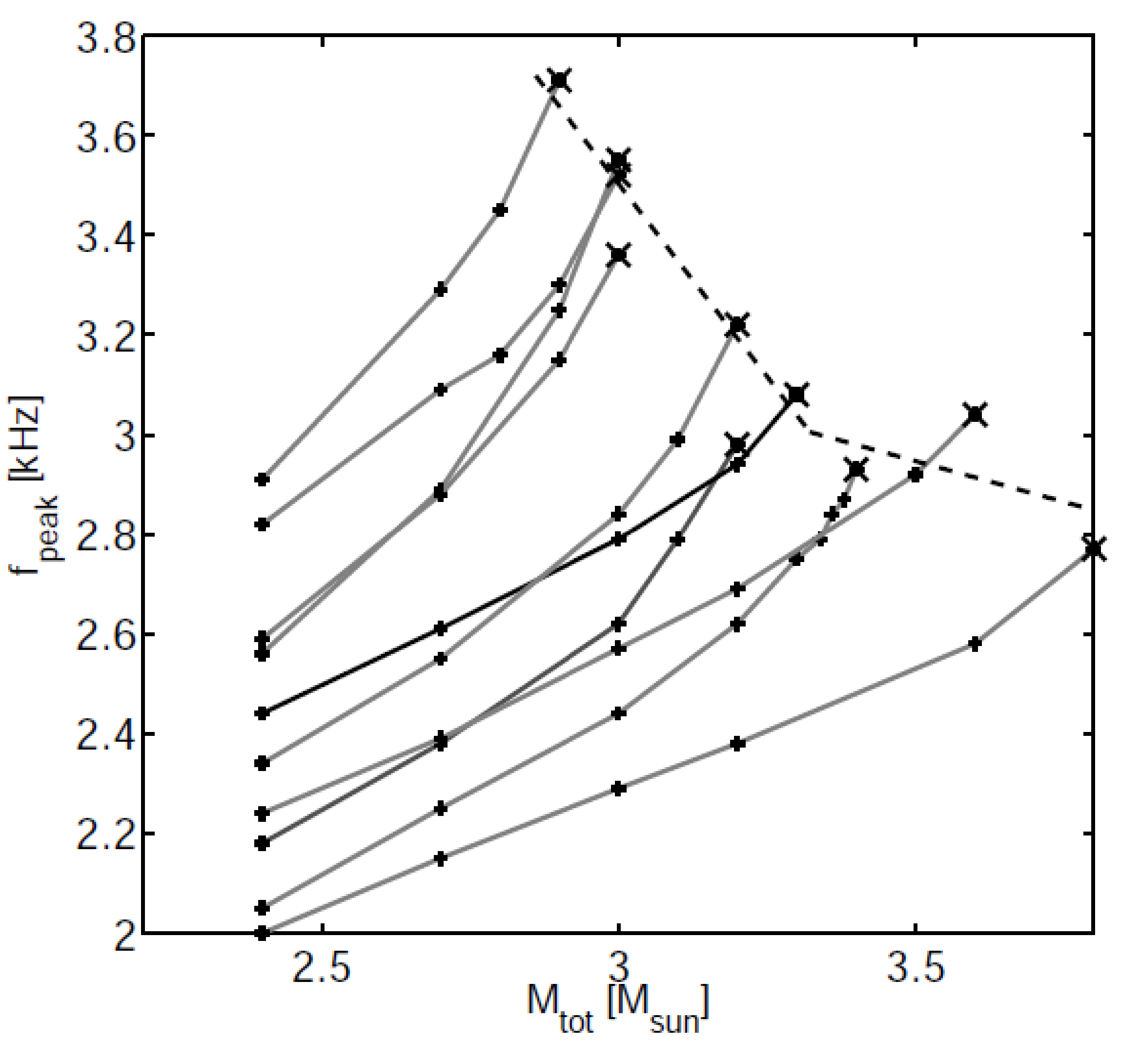

Details in Bauswein et al. 2014

Two f_{peak} measurements at different M_{tot} yield threshold mass and “threshold frequency” !!!

Extrapolation procedure

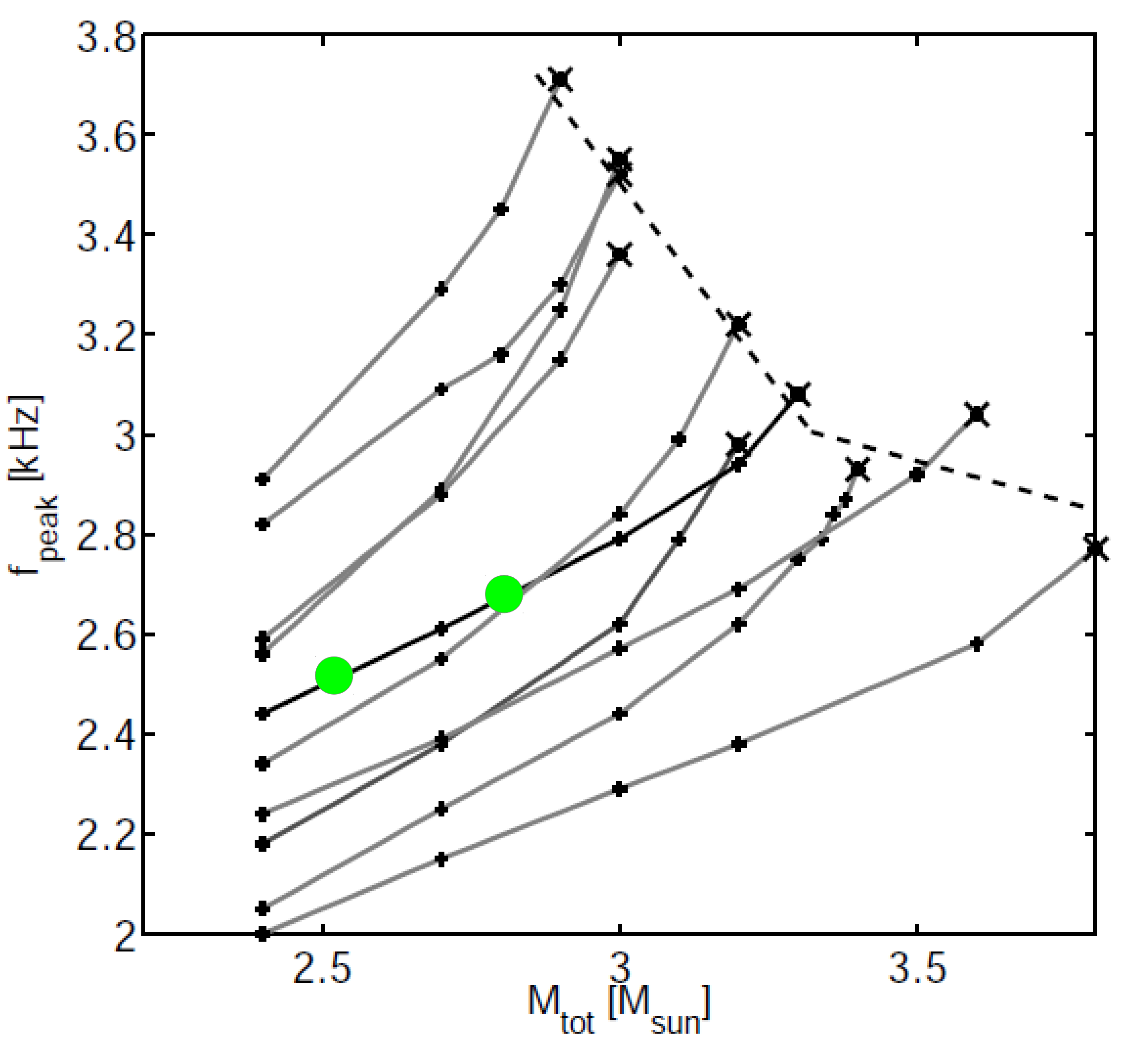

Details in Bauswein et al. 2014

Two f_{peak} measurements at different M_{tot} yield threshold mass and "threshold frequency" !!!

Extrapolation procedure

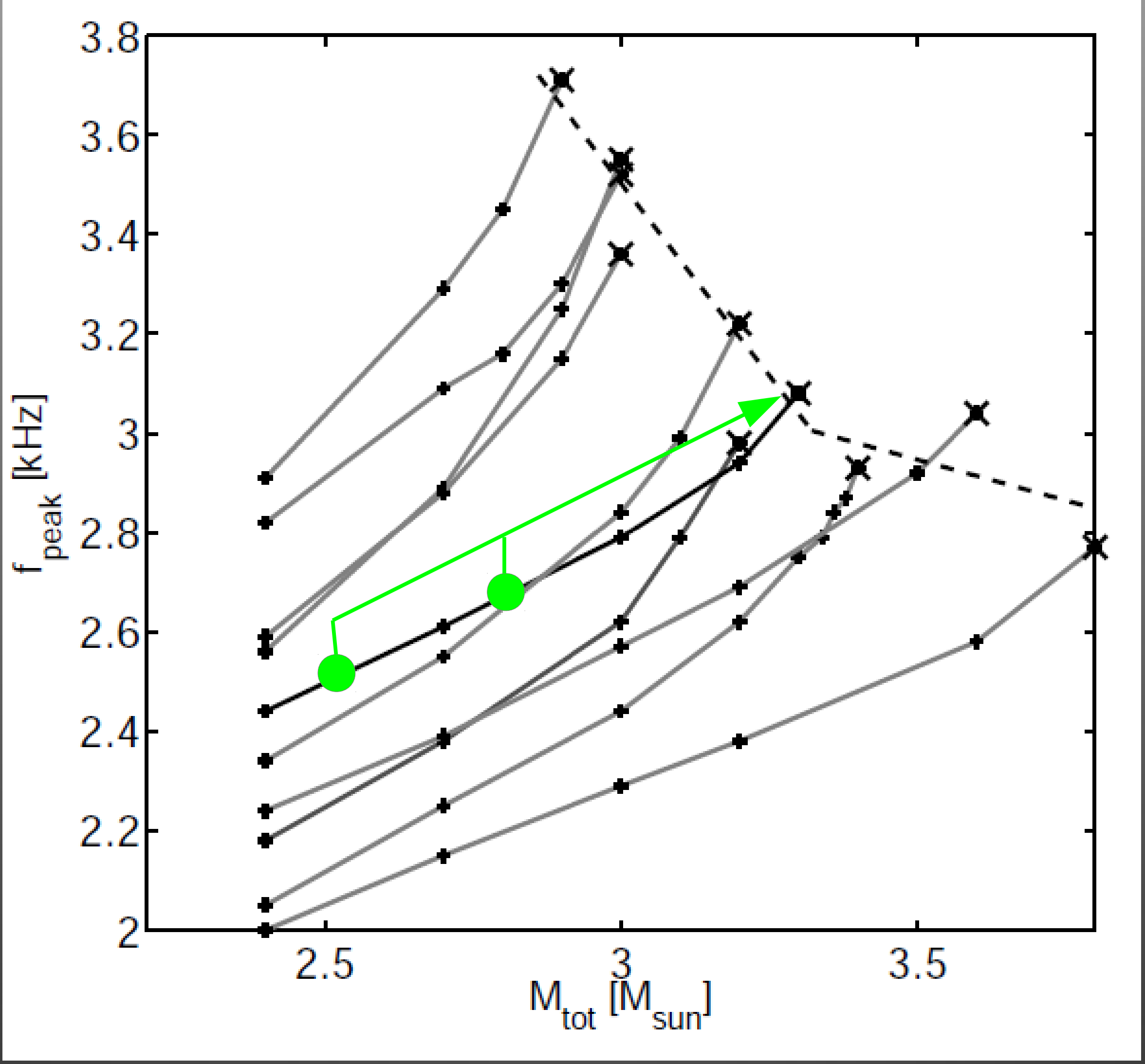

Details in Bauswein et al. 2014

Two f_{peak} measurements at different M_{tot} yield threshold mass and "threshold frequency" !!!

Two f_{peak} measurements at most common M_{tot} yield f_{thres} and M_{thres}

M_{thres}: highest binary mass which leads to a NS remnant (instead of direct BH collapse)

f_{thres}: oscillation frequency of this most massive NS merger remnant, so highest possible peak frequency

What can be learned from f_{thres} and M_{thres}?

R_{max} determination via extrapolation

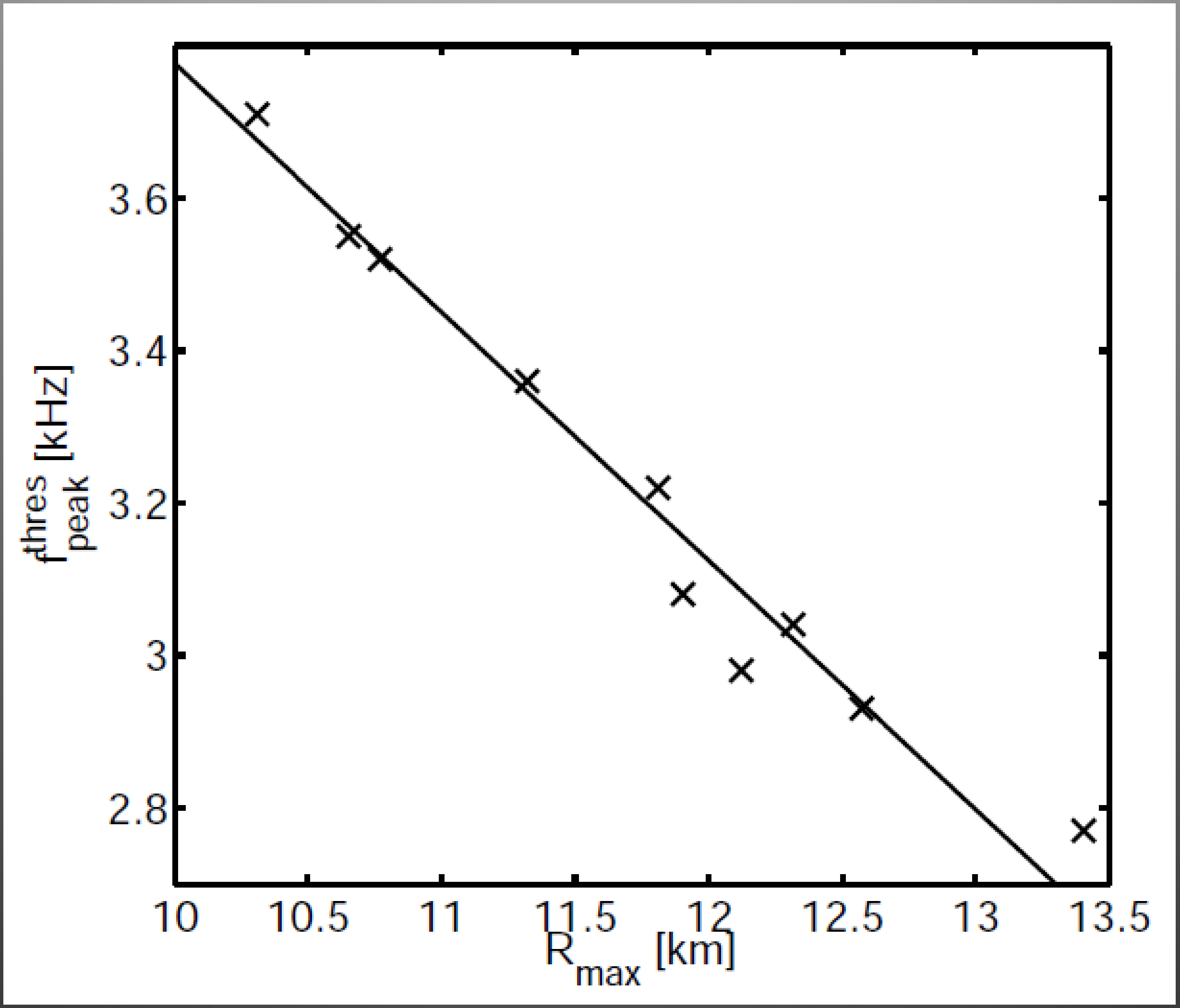

Threshold frequency f_{thres} yields a good estimate of the radius of the TOV maximum mass configuration (a few 100 meters)

Threshold mass

Likely to be related to M_{max} (maximum mass of nonrotating NSs)

M_{max} threshold for static, nonrotating NS

M_{thres} threshold for hot, differentially rotating NS (merger remnant)

$\longrightarrow$ $M_{thres} = k * M_{max}$

(k fractional increase)

Threshold mass – dependence on NS/EoS properties

Likely to be related to M_{max} (maximum mass of nonrotating NSs)

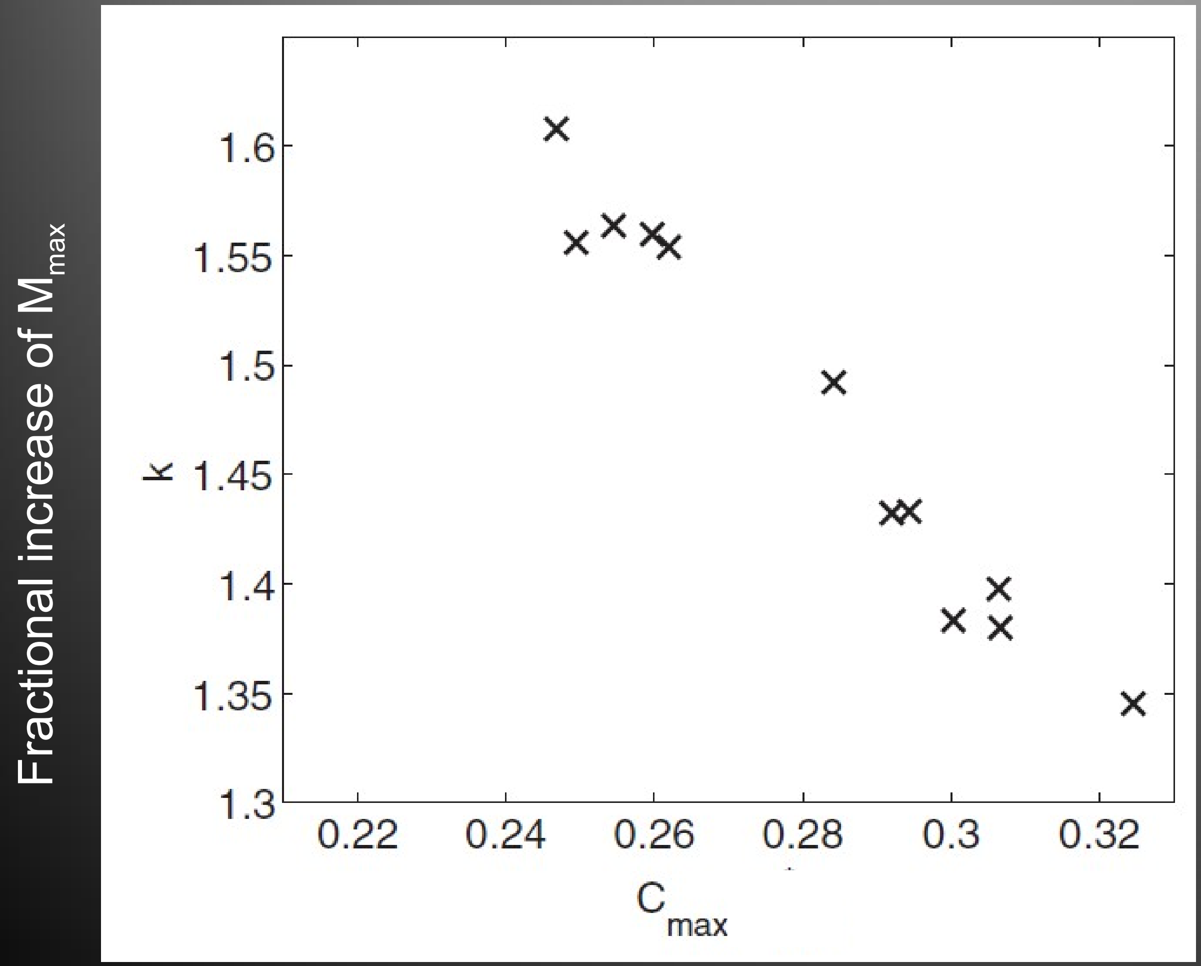

$$M_{thres} = k * M_{max}$$

with $k = k(C_{max})$

$$C_{max} = G\, M_{max} / (c^2\, R_{max})$$

(compactness of TOV maximum-mass configuration)

=> $M_{thres} = M_{thres}(M_{max}, R_{max})$

Bauswein et al. 2013

Threshold mass – dependence on NS/EoS properties

Likely to be related to M_{max} (maximum mass of nonrotating NSs)

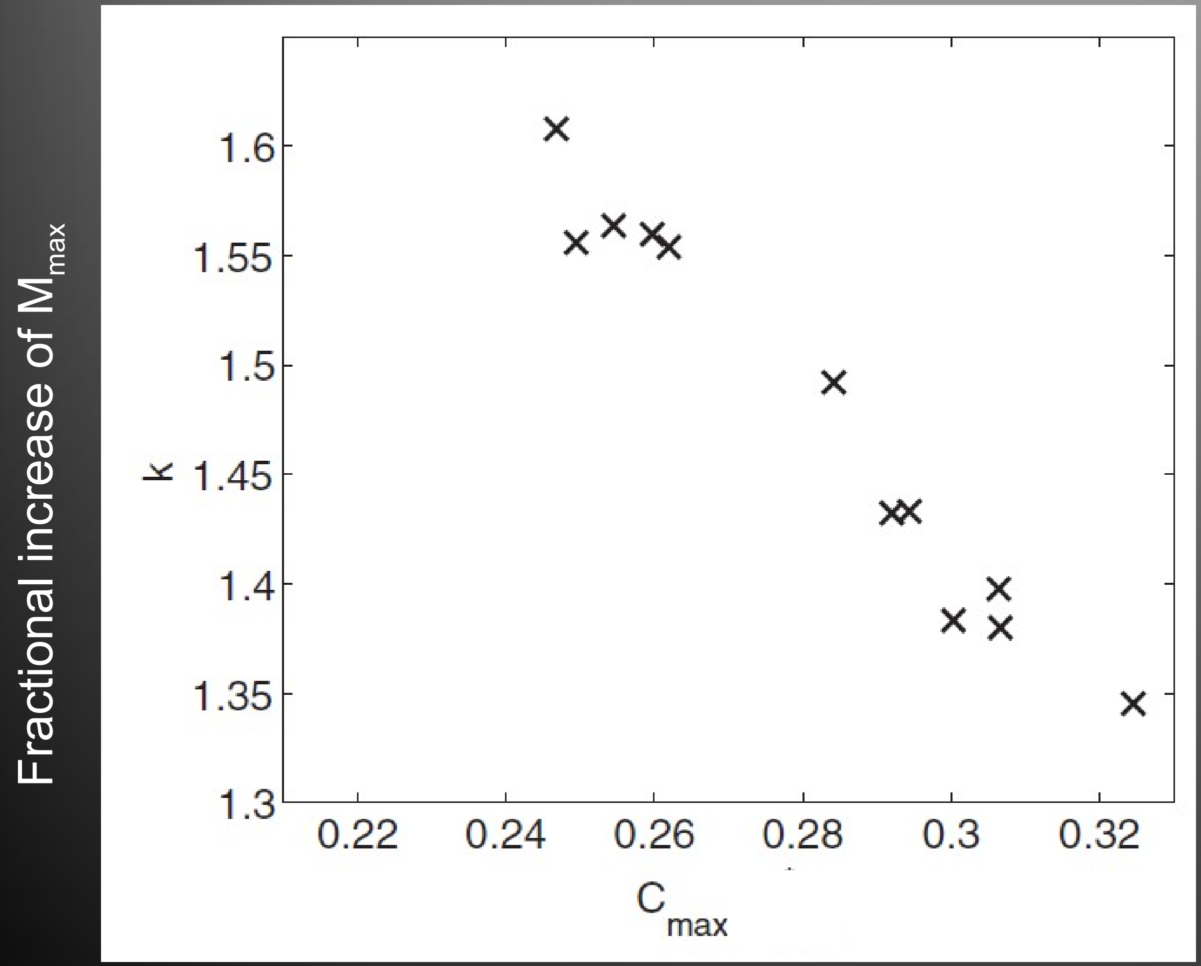

$$M_{thres} = k * M_{max}$$

with $k = k(C_{max})$

$$C_{max} = G\, M_{max} / (c^2\, R_{max})$$

(compactness of TOV maximum-mass configuration)

=> $M_{thres} = M_{thres}(M_{max}, R_{max})$

Bauswein et al. 2013

Threshold mass – dependence on NS/EoS properties

Likely to be related to M_{max} (maximum mass of nonrotating NSs)

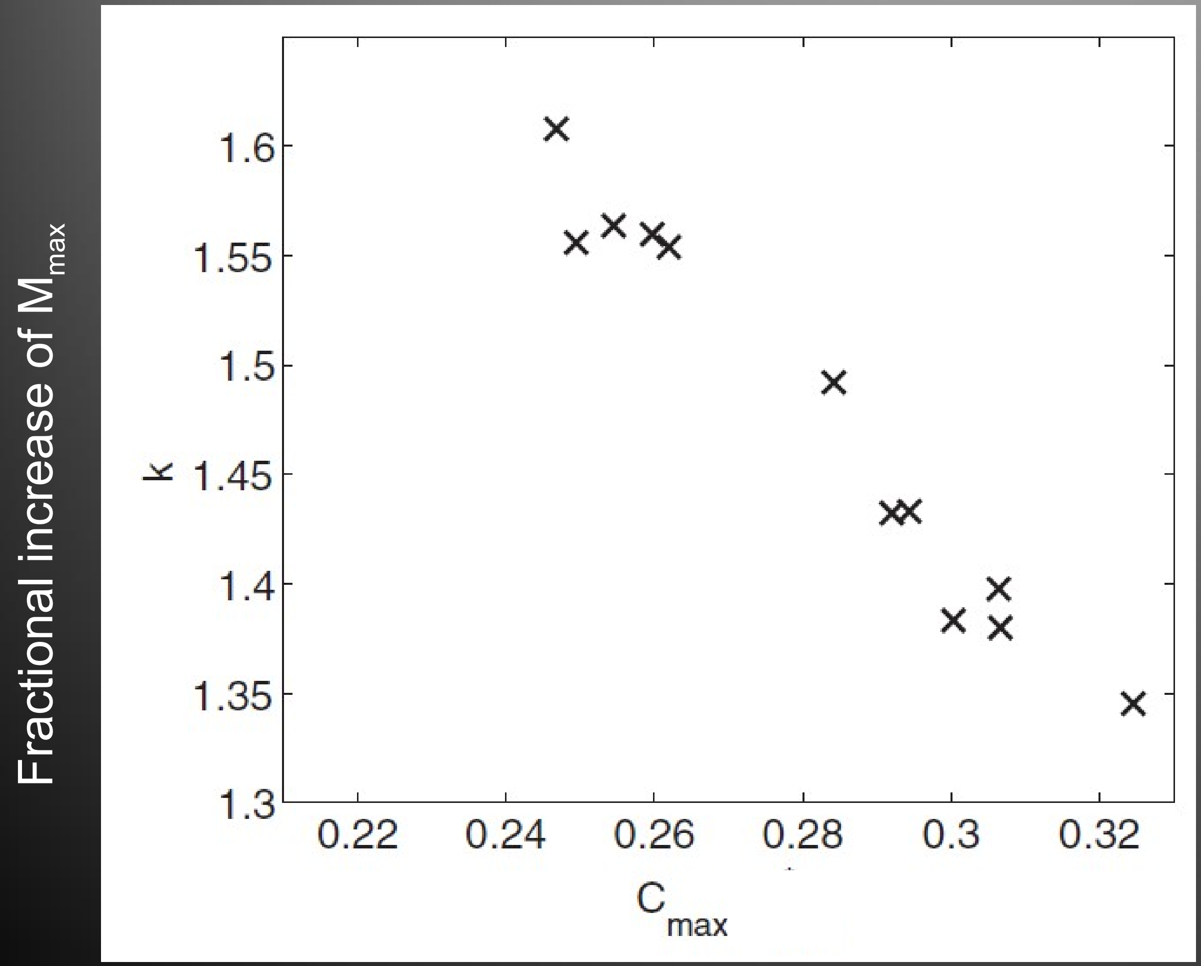

$$M_{thres} = k * M_{max}$$

with $k = k(C_{max})$

$$C_{max} = G\ M_{max} / (c^2\ R_{max})$$

(compactness of TOV maximum-mass configuration)

=> $M_{thres} = M_{thres}(M_{max}, R_{max})$

Bauswein et al. 2013

Maximum mass via extrapolation

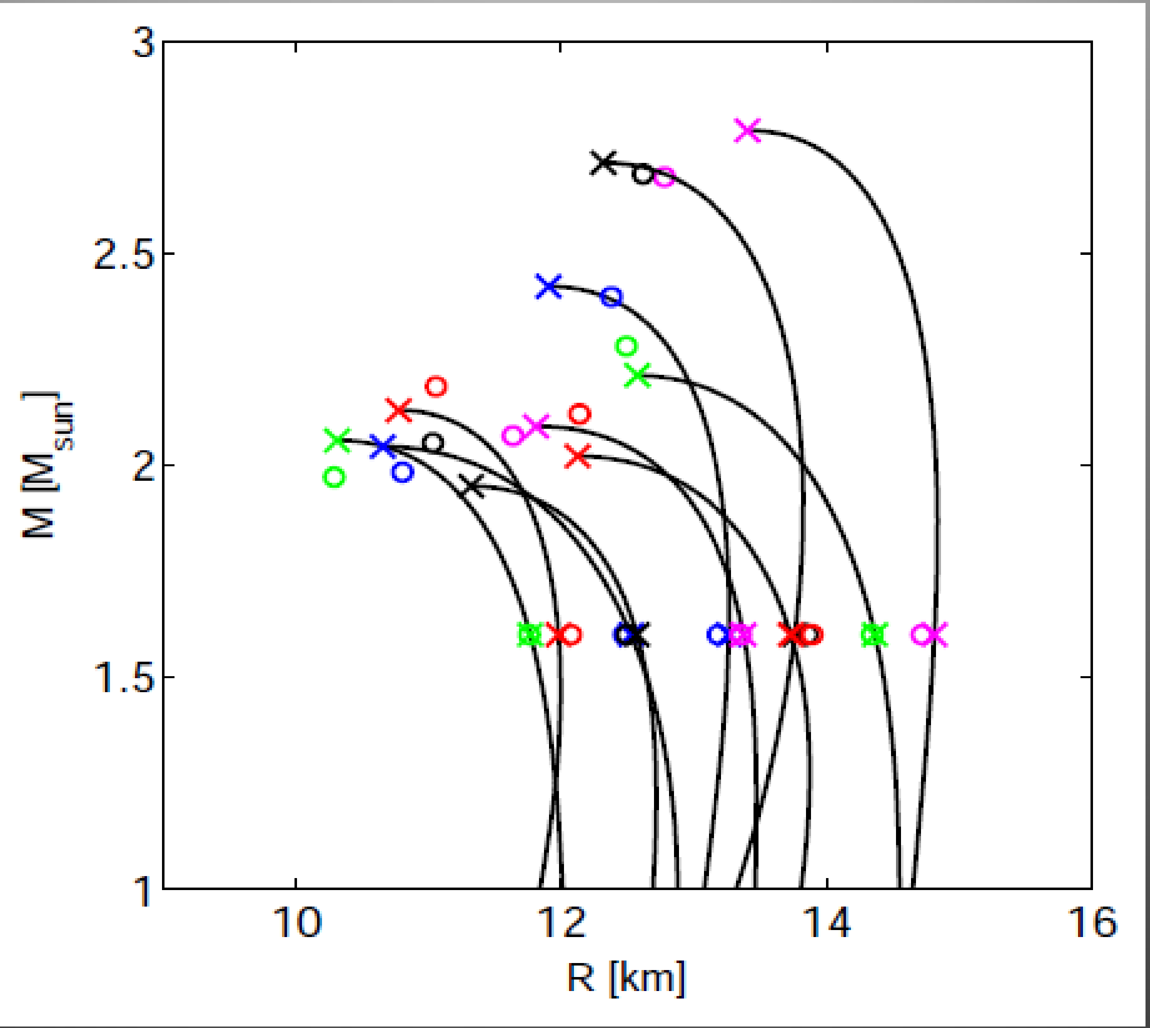

M_{max} within 0.1 M_{sun}, R_{max} within a few 100 m

(from f_{peak} detections at common M_{tot})

from two measurements of f_{peak} at moderate M_{tot}

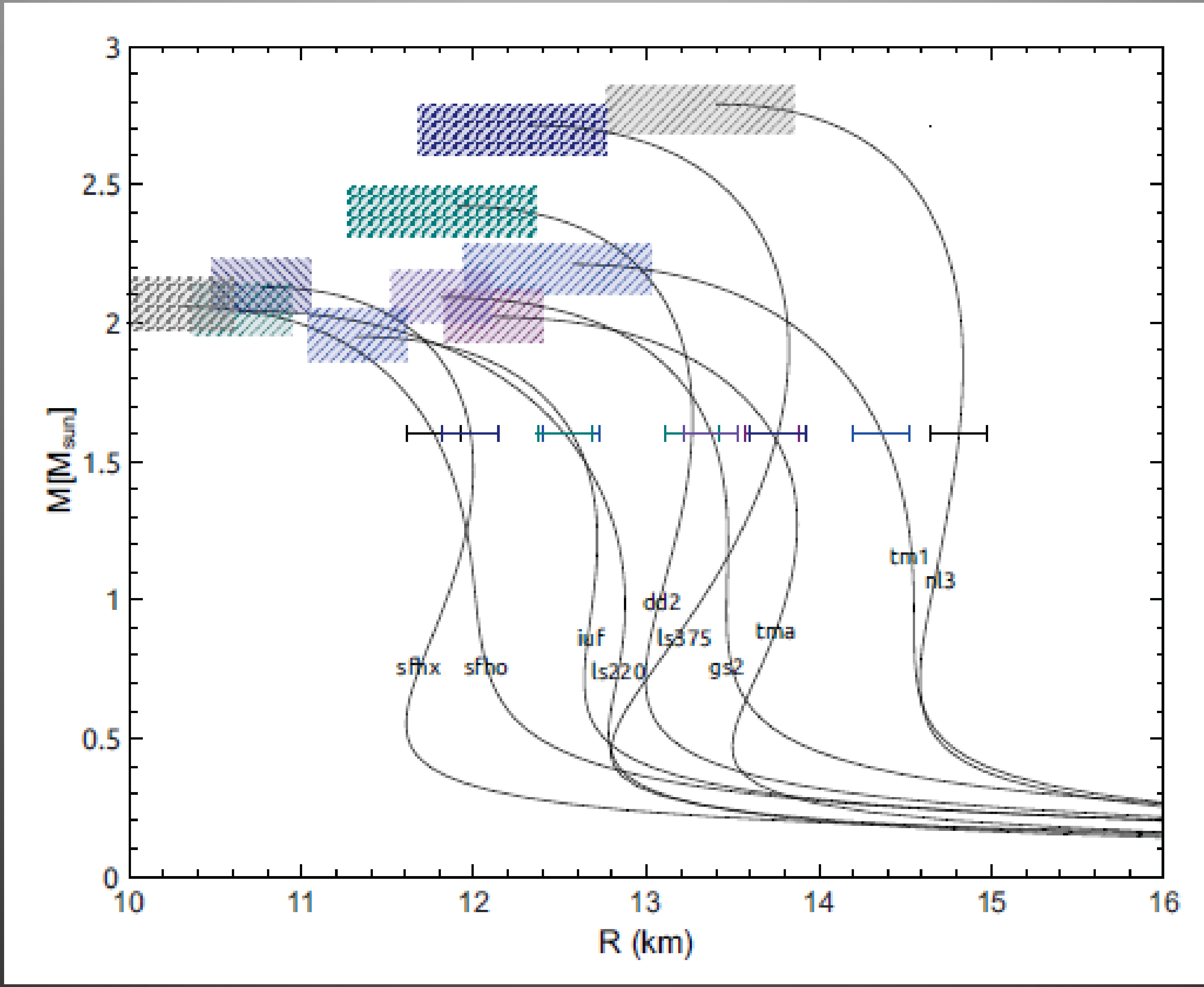

(final error will depend on EoS and extact systems measured)

Note: M_{thres} may also be constrained from prompt collapse directly

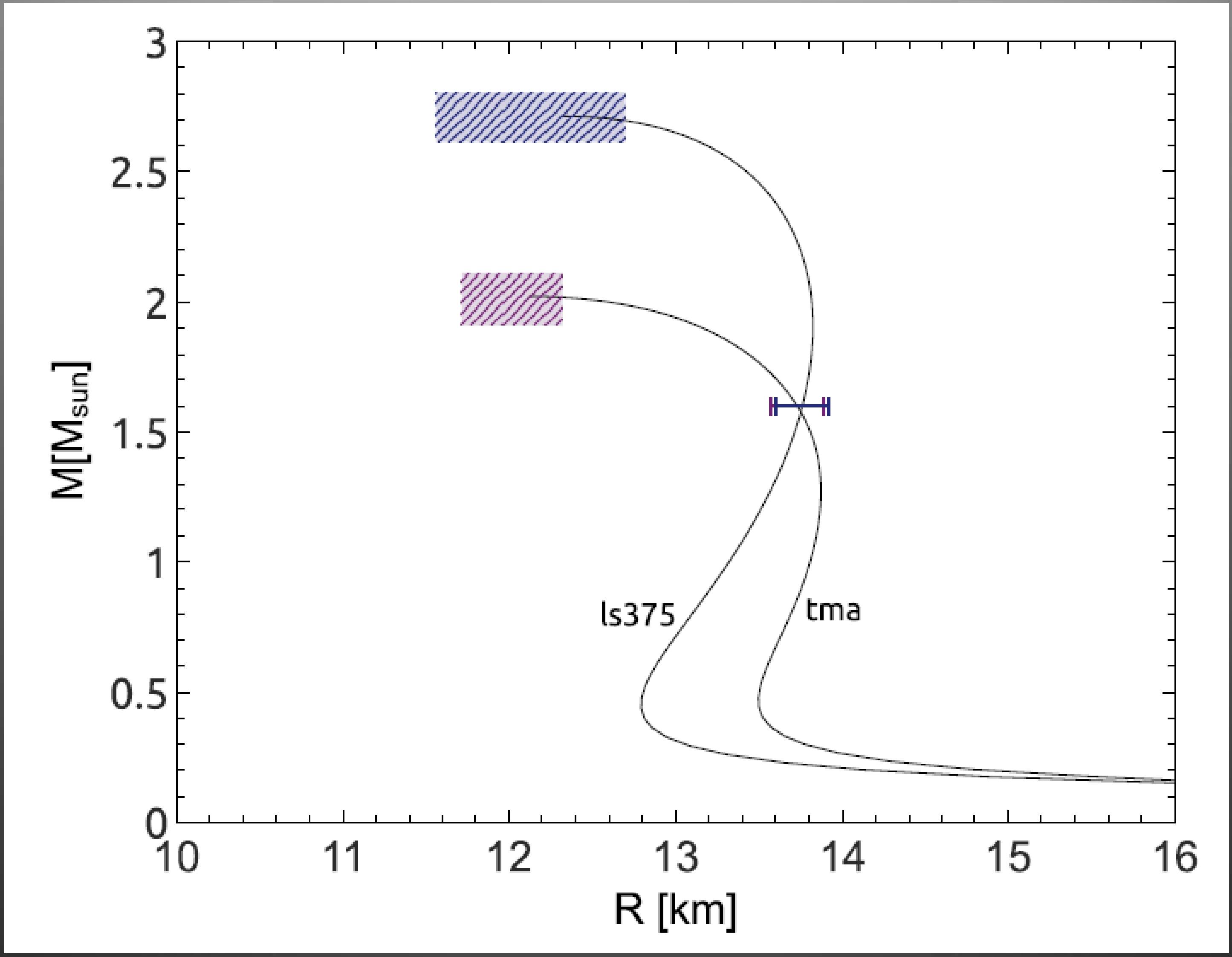

3
2.5
2
1.5
1
0.5
0
10
11
12
13
14
15
16
M[M_sun]
R [km]
ls375
tma

Maximum density via extrapolation

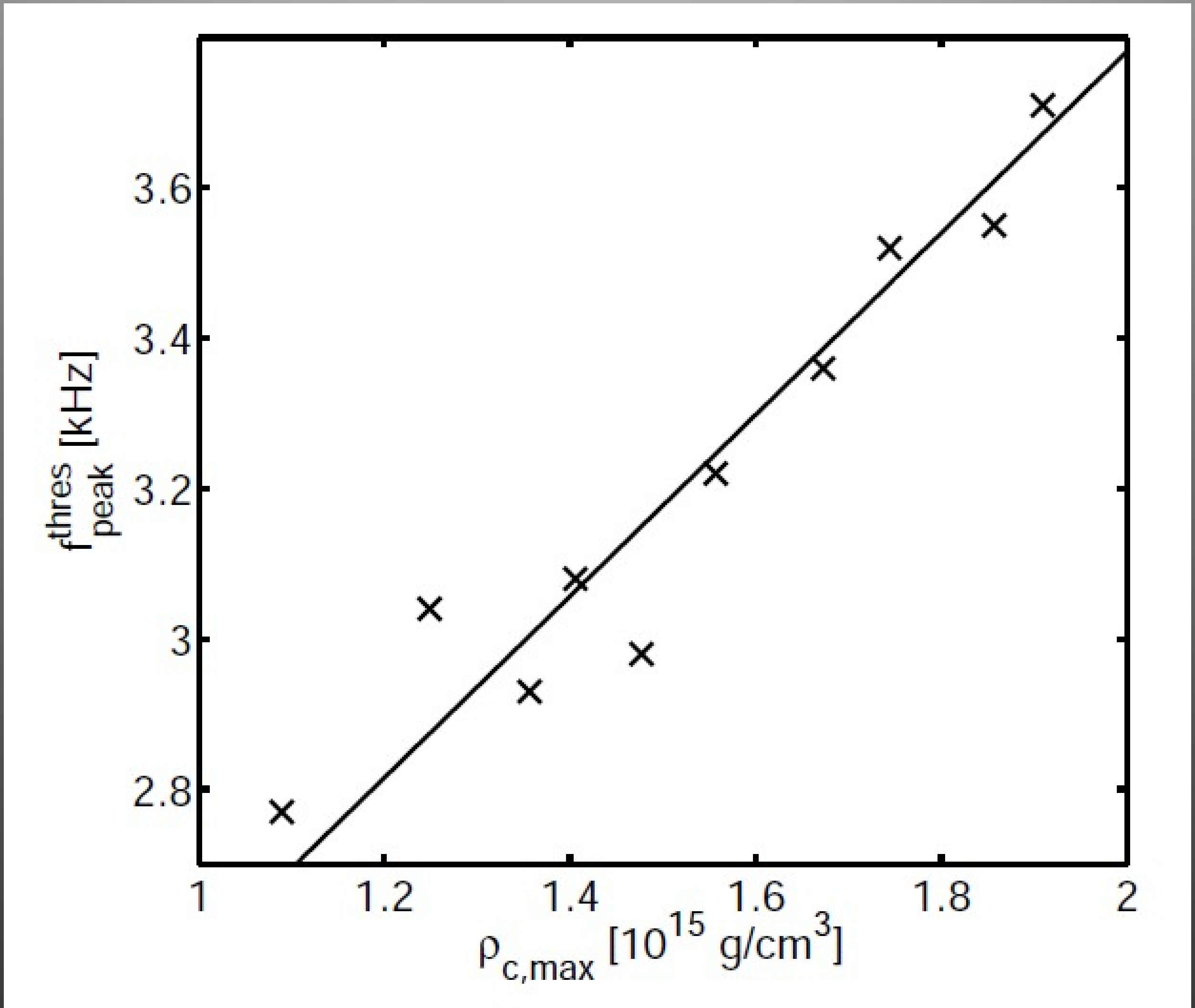

Maximum density of nonrotating NS within 10 per cent

Variation of binary parameter

M_1 and M_2 measurable from GW inspiral signal

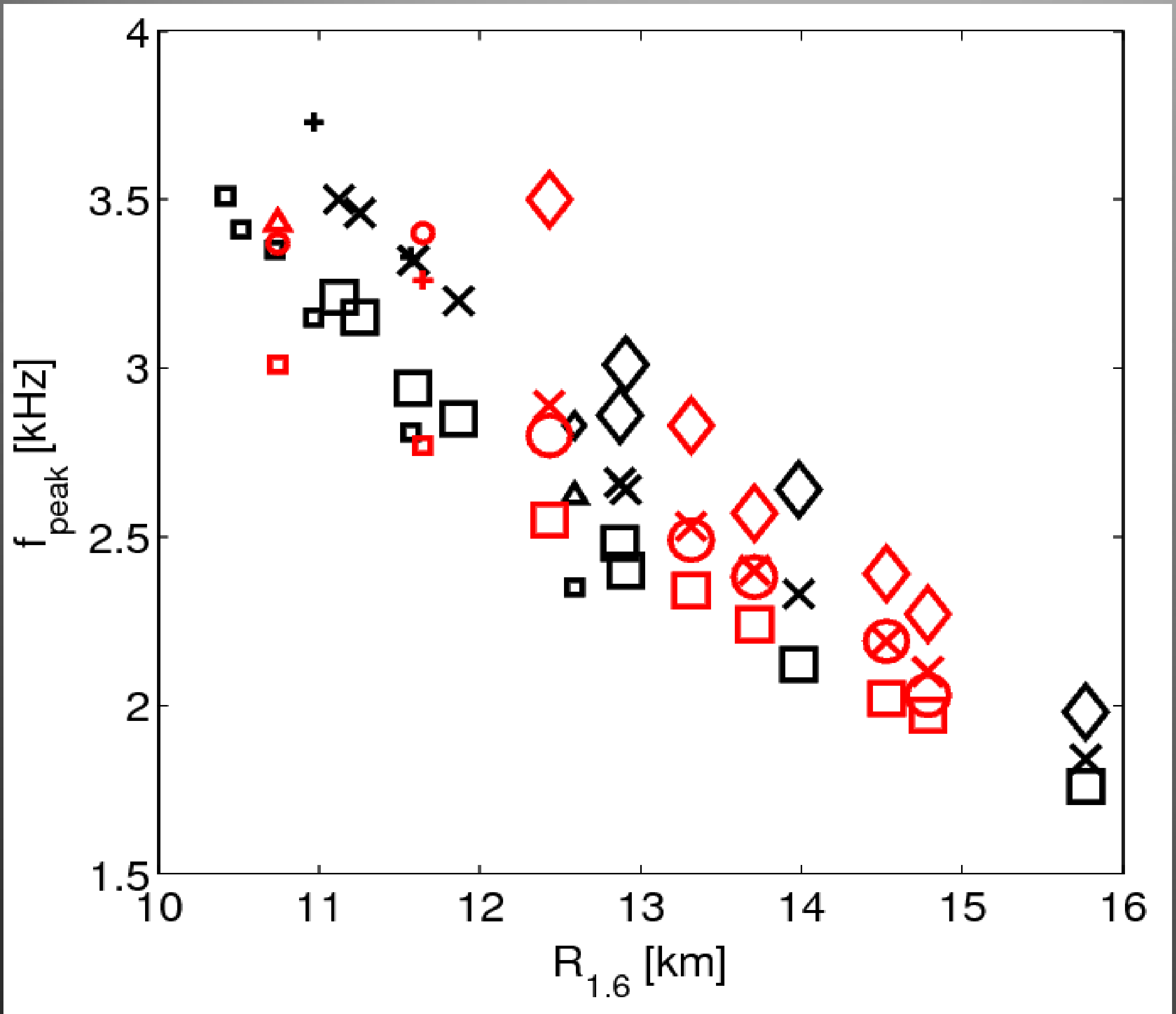

Squares: 1.2 - 1.2

Circles: 1.2 – 1.5

Crosses: 1.35 - 1.35

Diamonds: 1.5 - 1.5

Note: for the different total binary masses different radii of nonrotating NSs represent better choice (involved density regimes)

Collapse behavior of NS mergers

(prompt vs. delayed/stable)

and the maximum mass of nonrotating NSs

Estimates of maximum NS mass

Key quantity: Threshold binary mass M_{thres} for prompt BH collapse

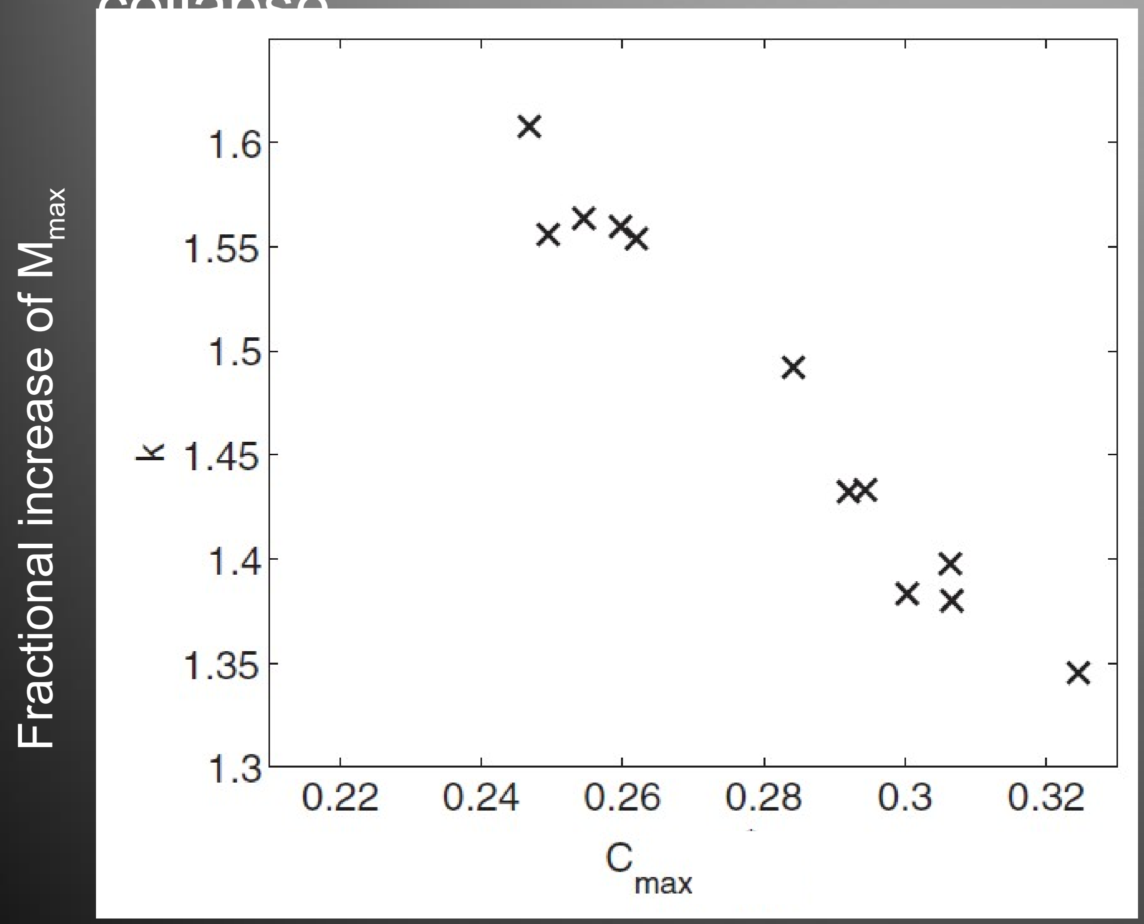

$$M_{thres} = k * M_{max}$$

with $k = k(C_{max})$

$$C_{max} = G M_{max} / (c^2 R_{max})$$

(compactness of TOV maximum-mass configuration)

=> $M_{thres} = M_{thres}(M_{max}, R_{max})$

Bauswein et al. 2013

$$k = \frac{M_{thres}}{M_{max}}$$

← From simulations with different M_{tot}

← TOV property of employed EoS

M_{max} estimates

observable

$$M_{thres} = M_{thres}(M_{max},R_{max}) = M_{thres}(M_{max},R_{1.6})$$

Pure TOV properties

<u>Two methods to determine M_{max}:</u>

- Determine M_{thres} by direct observations of delayed and prompt collapse for different M_{tot} (Bauswein et al. 2013)
- Extrapolate $f_{peak}(M_{tot}) \rightarrow f_{thres}(M_{thres})$ behavior from several events at lower binary masses (most likely range) (Bauswein et al. 2014)

from two measurements of f_{peak} at moderate M_{tot}

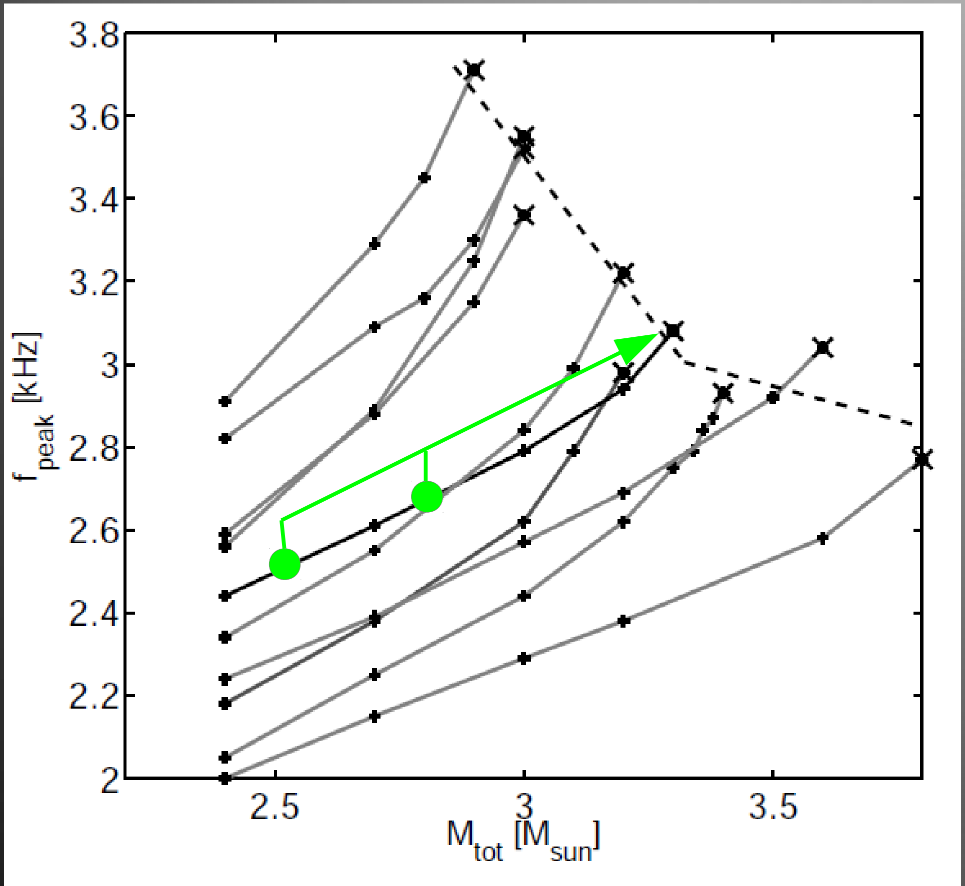

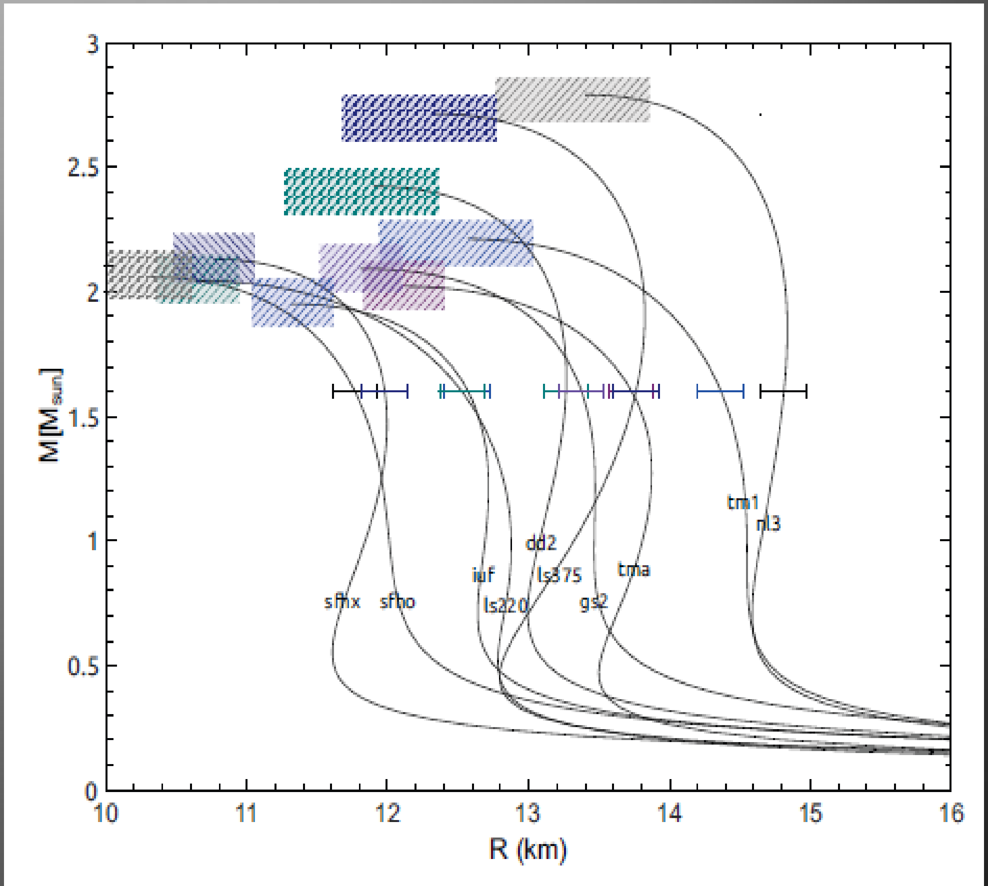

Bauswein et al. 2014

(final error will depend on EoS and exact systems measured)